


RESEARCH ARTICLE

Coupled C, H, N, S and Fe biogeochemical cycles operating in the continental deep subsurface of the Iberian Pyrite Belt

Ricardo Amils^{1,2}  | Cristina Escudero^{1,2} | Monike Oggerin¹ |
Fernando Puente Sánchez¹ | Alejandro Arce Rodríguez^{3,4} |
David Fernández Remolar¹ | Nuria Rodríguez¹ | Miriam García Villadangos¹ |
José Luis Sanz⁵ | Carlos Briones¹ | Mónica Sánchez-Román¹ |
Felipe Gómez¹ | Tania Leandro² | Mercedes Moreno-Paz¹ |
Olga Prieto-Ballesteros¹ | Antonio Molina¹ | Fernando Tornos¹ |
Irene Sánchez-Andrea⁶ | Kenneth Timmis³ | Dietmar H. Pieper⁴ | Victor Parro¹

¹Centro de Astrobiología (CSIC-INTA), Torrejón de Ardoz, Spain

²Centro de Biología Molecular Severo Ochoa (CSIC-UAM), Universidad Autónoma de Madrid, Madrid, Spain

³Institute of Microbiology, Technical University Braunschweig, Germany

⁴Microbial Interactions and Processes Research Group, Helmholtz Centre for Infection Research, Braunschweig, Germany

⁵Department of Molecular Biology, Universidad Autónoma de Madrid, Madrid, Spain

⁶Department of Microbiology, Wageningen University, Netherlands

Correspondence

Ricardo Amils, Centro de Biología Molecular Severo Ochoa, Universidad Autónoma de Madrid, Cantoblanco, Madrid 28049, Spain.
Email: ramils@cbm.csic.es

Present address

Monike Oggerin, Molecular Ecology Group, Max Plank Institute für Marine Mikrobiologie, Bremen, Germany.

Fernando Puente Sánchez, Department of Aquatic Science and Assessment, Swedish University of Agricultural Sciences (SLU), Uppsala, Sweden.

Alejandro Arce Rodríguez, Molecular Bacteriology Group, Helmholtz Zentrum für Infektionsforschung, Braunschweig, Germany.

David Fernández Remolar, National Space Science and Technology Center, United Arab Emirates University, Al Ain, UAE.

Mónica Sánchez-Román, Earth Science Department, Vrije Universiteit Amsterdam, the Netherlands.

Tania Leandro, Institute for Bioengineering and Bioscience (IBB), Instituto Técnico, Lisbon, Portugal.

Abstract

Microbial activity is a major contributor to the biogeochemical cycles that make up the life support system of planet Earth. A 613 m deep geomicrobiological perforation and a systematic multi-analytical characterization revealed an unexpected diversity associated with the rock matrix microbiome that operates in the subsurface of the Iberian Pyrite Belt (IPB). Members of 1 class and 16 genera were deemed the most representative microorganisms of the IPB deep subsurface and selected for a deeper analysis. The use of fluorescence in situ hybridization allowed not only the identification of microorganisms but also the detection of novel activities in the subsurface such as anaerobic ammonium oxidation (ANAMMOX) and anaerobic methane oxidation, the co-occurrence of microorganisms able to maintain complementary metabolic activities and the existence of biofilms. The use of enrichment cultures sensed the presence of five different complementary metabolic activities along the length of the borehole and isolated 29 bacterial species. Genomic analysis of nine isolates identified the genes involved in the complete operation of the light-independent coupled C, H, N, S and Fe biogeochemical cycles. This study revealed the importance of nitrate reduction microorganisms in the oxidation of iron in the anoxic conditions existing in the subsurface of the IPB.

This is an open access article under the terms of the [Creative Commons Attribution-NonCommercial-NoDerivs](https://creativecommons.org/licenses/by-nc-nd/4.0/) License, which permits use and distribution in any medium, provided the original work is properly cited, the use is non-commercial and no modifications or adaptations are made.

© 2022 The Authors. *Environmental Microbiology* published by Applied Microbiology International and John Wiley & Sons Ltd.

Fernando Tornos, Instituto de Geociencias,
Universidad Complutense de Madrid, Madrid,
Spain.

Funding information

FP7 Ideas: European Research Council,
Grant/Award Number: ERC Advanced Grant
#250-350

INTRODUCTION

Rock continental subsurface geomicrobiology, which seeks to understand how life is sustained in the resource-poor confines of rock matrices lacking solar radiation inputs, is a new research frontier (Colman et al., 2017; Escudero, Oggerin, & Amils, 2018; Gold, 1992; Magnabosco et al., 2018; Pedersen, 1993). Subsurface ecosystems are also instructive for astrobiology, as models for both the origin of life in putative early Earth scenarios (Pedersen, 2000) and for assessing potential subsurface life in other planetary bodies (Boston et al., 1992; Purkamo et al., 2020). Although Charles Darwin predicted the existence of subsurface life almost 200 years ago (Darwin, 1839), and a few pioneering early 20th century observations suggested the existence of active microorganisms in the subsurface (Bastin et al., 1926; Zobell, 1938), the first report describing the results of a dedicated continental rock matrix drilling was published relatively recently (Zhang et al., 2005). Most studies on continental subsurface microbial diversity are based on the analysis of groundwater samples (Chapelle et al., 2002; Momper, Reese, et al., 2017; Nuppenen-Puputti et al., 2022; Purkamo et al., 2018; Sherwood Lollar et al., 2019; Stevens & McKinley, 1995; Suzuki et al., 2013; Wu et al., 2016), which, although providing useful microbiological diversity information, cannot directly relate it to the pertinent geological features of the complex subsurface solid matrix which the microorganisms inhabit. Despite recent progress in the field (Cabugao et al., 2022; Dutta et al., 2018; Purkamo et al., 2020; Soares et al., 2019), information concerning the abundance, diversity and ecophysiological integration of extant microbial species, as well as microbiome function, connectivity and sustainability, in continental subsurface rock ecosystems is still scarce.

The Iberian Pyrite Belt (IPB) stretching for some 250 km across SW Iberian Peninsula hosts the largest concentration of volcanogenic massive metal sulfide deposits and arguably the largest sulfide anomaly in the Earth's crust (Barriga, 1990; Tornos, 2006). Its formation through hydrothermalism took place during the Hercynian orogenesis (Barriga, 1990; Lescuyer et al., 1998). Río Tinto is a 92 km long river with its source in Peña de Hierro, in the core of the IPB, which flows into the Atlantic Ocean at Huelva. The Río Tinto is an unusual extreme environment due to its acidity and high concentration of heavy metals, as well as its

high level of microbial diversity (Amaral-Zettler et al., 2002; Amils, 2016; González-Toril et al., 2003). It has been generally assumed that the extreme conditions found in the Río Tinto basin were the result of 5000 years of mining activity in the area (Alvarez & Nieto, 2015; Leblanc et al., 2000; van Geen et al., 1997). However, recent geophysical, hydrogeological, and other geological data suggest that the IPB subsurface acts as a huge underground reactor, in which sulfidic minerals are the main energy source and the metabolic reaction products drain to the river (Allman et al., 2021; Gómez-Ortiz et al., 2014). Here, we report a detailed multidisciplinary analysis of the microbiology and microbially driven geochemical processes operating in the deep subsurface rock matrix of the IPB. The results allowed the identification of the most representative microorganisms, which are able to carry out the light independent, coupled C, H, N, S and Fe biogeochemical cycles. Enrichment cultures have been used to identify the most characteristic metabolic activities operating in the deep subsurface of the IPB. The analysis of the genomes of nine isolates from the enrichment cultures identified the presence of genes involved in the operation of the biogeochemical cycles and highlighted the role of the nitrogen cycle and the nitrate-reducing microorganisms in the anoxic conditions existing in the subsurface of the IPB.

EXPERIMENTAL PROCEDURES

Drilling and sampling processing

Borehole BH10 was continuously cored by rotary diamond-bit drilling on lexan liners using a Boart Longyear HQ wireline system producing 3 m of 60 mm diameter cores. Potable drinking water was used as a drilling fluid to lubricate the bit and return cuttings to the surface. When required FT Bentonil A, SC MUD P and SC VIS HVL polymers from Süd-Chemie España S.L. were used to facilitate the drilling. The European Community (EC) and Chemical Abstract Service (CAS) codes for these polymers guaranty that they do not produce acetate or butyrate as degradation products. Fluids were recirculated. To detect potential contamination of samples, sodium bromide (10 mg/L) was added to the drilling fluid as a marker. A preliminary survey of outcrop samples from the area suggested that background Br^- was negligible. Upon retrieval from the

drilling rig, cores were divided into 60 cm-length pieces and inspected for signs of alteration. Selected cores were deposited in plastic bags, oxygen was displaced with N_2 , sealed and transported to a field laboratory located at the Museo Minero in Riotinto village, close to the drilling site (2 km). Cores were stored in boxes for permanent storage and curation in the Instituto Geológico y Minero de España lithoteque in Pañarroya (Córdoba, Spain).

Upon arrival at the field laboratory, cores were placed in an anaerobic chamber (5% H_2 , 95% N_2 , <50 ppm O_2), logged and photographed. The anaerobic chamber and the airlock were decontaminated daily with Virkon S (Antec International Limited), a mixture of surfactants, organic acids, and strong oxidizers with the ability to disrupt bacterial membranes and degrade their nucleic acids. Furthermore, the chamber and the airlock were cleaned with a 50:50 bleach: water solution and ethanol before the introduction of a new core sample. Aseptic subsamples were obtained by splitting cores with a hydraulic press and drilling out the central untouched face with a rotary hammer drill mill cutter to produce powdered samples using sterile bits. Temperature of the hand drilling was strictly controlled with an infrared thermometer (maximum allowed drilling temperature 40°C). Samples for different analysis were sealed in gas-tight containers before removal from the anaerobic chamber. Mineralogical analysis was performed on pieces adjacent to the aseptic subsample.

Physicochemical characterization of rock core samples

Quantitative elemental analysis (C, H, N and S) of powdered samples was measured in duplicate in a LECO CHNS-932 (model 601-800-500) instrument. For inductively coupled plasma mass spectrometry (ICP-MS) and total reflection x-ray fluorescence (TXRF) analysis of powdered samples, a total acidic extraction was carried out according to the EPA 3052 microwave-assisted acid digestion of siliceous and organical-based matrixes method, using ultrapure HNO_3 , HF, HCl, H_2O_2 mixture (9:4:1:2) from Merck. The digestion was done in an Ethos Touch Control Screen of Milestone in high pressure and temperature-resistant containers at 220°C. For ICP-MS analysis, a NexION 2000 (PerkinElmer, USA) instrument was used. A multielemental semi-quantitative analysis was performed and ARD-01, lot #208, was used as matrix reference. All the analyses were performed in mode KED to avoid polyatomic interferences. For TXRF analysis, a TXRF S2 PicoFox instrument (Bruker, USA) with fix geometry was used. The mineral components of the material were determined by powder x-ray diffraction using a Seifert 3003 TT instrument (Materialkunde, Belgium) with $Cu K\alpha$ radiation ($\lambda = 1.542 \text{ \AA}$). The x-ray generator was set to an acceleration voltage of 40 kV and a filament

emission of 40 mA. Samples were scanned between 5° (2 θ) and 60° (2 θ) using a step size of 0.05° (2 θ) and a count time of 1 s.

Generation and analysis of rock sample leachates

Rock leachates were produced by adding 20 ml of sterile anoxic water to 10 g powdered core subsamples, incubating with a gentle stirring for 1 h at room temperature followed by centrifugation for 1 min at 10,000 rpm. The concentrations of inorganic anions and small molecular weight organic acids in the rock leachates were analysed by ion chromatography (Parro et al., 2011). The pH of the water solutions was measured with an inoLab pH metre WTW (GmbH, Germany) after 24 h of solution stabilization. Fe^{2+} and Fe^{3+} were determined using the Reflectoquant test (Merk Millipore, Spain), and NH_4^+ using a DR6000 spectrophotometer and the reaction kit LCK304 (HACH, USA) following the manufacturer's instructions. Total protein and sugar content were determined as follows: 1 g of sample (powder) was subjected to $3 \times 1 \text{ min}$ ultrasonic cycles in 2 ml of distilled water with 1–2 min stops by using a sonicator (Dr. Hielscher 50W DRH-UP50H sonicator, Hielscher Ultrasonics, Germany). Samples were centrifuged at 2000g to sediment the mineral particles, and the supernatants were directly assayed for protein concentration using the bicinchonitic acid protein assay reagent (Pierce, USA) (Smith et al., 1985) and sugar content as described by Dubois et al. (1956), respectively. A NanoDropp (NanoDrop Int., USA) instrument was used for spectrophotometric measurements.

Sandwich microarray immunoassays with LDChip300

Sandwich-type microarray immunoassays (LDChip300) were performed as described previously (Parro et al., 2011). Briefly, printed microscope slides with LDChip300 antibody microarray were blocked with 0.5 M Tris–HCl in 5% BSA for 5 min and then in 0.5 M Tris–HCl with 2% BSA for 30 min. After washing with TBSTRR buffer (0.4 M Tris–HCl pH 8, 0.3 M NaCl, 0.1% Tween 20) and drying the chip with quick centrifugation, the slides were mounted on a portable multiarray analysis module (MAAM) cassette for nine samples. Approximately, 0.5 g of ground core sample was resuspended in 2 ml of TBSTRR and sonicated ($3 \times 1 \text{ min}$ cycle) with a handheld Ultrasonic Processor (UP50H; Hielscher Ultrasonics, Germany). Coarse material was removed by filtering through 10- μm nylon filter and 50 ml of the extracts were injected into each MAAM chamber and incubated for 1 h with the LDChip300 at ambient temperature. After a wash with TBSTRR, the chips were incubated with a fluorescently

labelled antibody mixture for 1 h. The slides were then washed, dried, and scanned for fluorescence at 635 nm in a GenePix4100A scanner. Buffer was used as a blank control sample in parallel immunoassays. The scanned images were analysed with the GenePix Pro software (Genomic Solutions, USA). The final fluorescence intensity was quantified as previously reported (Parro et al., 2011).

Oligonucleotide microarray hybridization (PAM)

Oligonucleotide microarrays containing specific probes for prokaryotic microorganisms (PAM) were printed and treated as described (Garrido et al., 2008). Briefly, fluorescently labelled 16S rRNA amplicons were checked by agarose gel electrophoresis, then purified with Qiagen PCR Purification Kit columns (Qiagen, Germany) and set to hybridize in Hiblt hybridization buffer (Arrayit Corp., USA) at 50°C for 12 h in a water bath. They were then washed and scanned for fluorescence as previously described (Garrido et al., 2008).

DNA extraction and amplification

DNA extraction and amplification was done in the conditions described by Puente-Sánchez et al. (2018). Briefly, DNA extraction was performed in a UV- and ethanol-sterilized flow chamber. A 0.5 g of powdered core samples was introduced into a Ultra-Clean Bead Tube (MoBio Laboratories, USA), whose original buffer had been previously removed and substituted with 1 ml of phosphate buffer (1 M sodium phosphate, 15% ethanol). After adding 60 µl of MoBio Ultra-Clean Soil DNA solution S1, tubes were subjected to two FastPrep (MP Biomedicals, USA) cycles (30 s each, power setting of 5.5 m/s) separated by 1 min of ice cooling. Subsequently, tubes were incubated in a thermomixer at 80°C for 40 min, while shaking at 300 rpm. The MoBio Ultra-Clean Soil DNA extraction protocol was then followed by the addition of solution S2 according to the manufacturer's instructions. All materials and stock solutions were UV sterilized for 5 min either in GS Linker UV Chamber (Bio-Rad Laboratories, Spain) or in Stratalinker 1800 UV crosslinker (Stratagene, USA) to eliminate trace DNA contaminations. The isolated DNA was later subjected to multiple displacement amplification (MDA) using either MagniPhi Phi29 polymerase (Genetrix, Spain) or the REPLI-g Single Cell Kit (Qiagen, Germany). The non-enzymatic MDA reagents and the random hexamers were decontaminated as described (Woyke et al., 2011). The resulting AMD amplification products were finally purified using a MicroSpin G-50 column (GE Healthcare, Spain). Successful amplification was confirmed by PCR of the 16S rRNA gene. Negative controls were also run from MDA

reagents without template DNA. Furthermore, in the cases where the MDA-amplified DNA gave no 16S PCR product, another nine individual rounds of DNA isolation were performed using the same extraction protocol (for a total of around 5 g of powdered core sample). The 10 DNA isolations from the same rock core sample were immediately pooled, cleaned with phenol:chloroform:isoamyl alcohol (25:24:1) and precipitated with 70% ethanol (also UV sterilized) as described elsewhere. The DNA pellet was finally eluted in 50 µl of 10 mM Tris pH 8.0, amplified by MDA and purified using the MicroSpin G-50 columns. Additionally, an upscaled modification of the previous protocol was applied to a set of samples using the PowerMax Soil DNA Isolation Kit (MoBio Laboratories, USA). A total of 15 ml of phosphate was mixed with up to 10 g of powdered core sample into the provided PowerMax Bead Tube. After the addition of 5 ml of PowerMax Soil DNA solution C1, the tubes were vortexed vigorously for 30 s and subjected to two FastPrep cycles (40 s, power setting of 6.0 m/s). Samples were then incubated at 80°C in a water bath during 40 min and centrifuged at 2500 g for 3 min at room temperature. The supernatant was recovered in a new collection tube and the protocol was followed by the addition of solution C2. Once again, the solutions employed were UV sterilized as described above, and the resulting DNA was also subjected to MDA amplification, purification, and PCR of the 16S rRNA gene.

DNA was additionally isolated from a drilling water sample, to trace potential contamination events occurring during the core retrieval process. Two 250 ml drill cooling water samples, collected with 15 days difference, were pooled and filtered through a 0.22-µm pore-size filter (Millipore, Germany). The filter was introduced into an empty Ultra-Clean Bead Tube and the DNA was isolated using the protocol described above. Additionally, during the preparation of the aliquots used for MiSeq sequencing (see below) DNA was also extracted from an empty PowerMax Bead Tube to account also for laboratory contaminations during extraction of the nucleic acids (DNA isolation control). DNA was finally eluted in 50 µl of 10 mM Tris-HCl buffer and quantified using a NanoDrop spectrophotometer. The V5–V6 hypervariable regions of the bacterial 16S rRNA gene were PCR amplified using primers 807F and 1050R (Bohorquez et al., 2012). The barcoding of the DNA amplicons, as well as the addition of Illumina adaptors, was carried out as described previously (Camarinha-Silva et al., 2014).

Generation of Illumina amplicon libraries and community profiling

The conditions described by Puente-Sánchez et al. (2018) were followed. Briefly, the PCR-generated amplicon libraries were sent for 250-nt paired-end

sequencing on a Illumina MiSeq platform at the Genome Analytic platform of the Helholtz Centre for Infection Research. For the construction of metagenomic libraries, 0.8 µg of amplified DNA was mixed with 1× fragmentase reaction buffer in a final volume of 18 µl, vortexed thoroughly, and incubated on ice for 5 min. The fragmentation reaction was then started by mixing the samples with 2 µl of NEBNext dsDNA fragmentase (New England Biolabs Inc., USA) and carried out for 25 min at 37°C. After incubation, the fragmentation was halted by the addition of 5 µl of 0.5 M EDTA. The ensuing DNA was purified with the QIAquick PCR Purification Kit (Qiagen, Germany) and eluted in a final volume of 35 µl before quantification with a Nanodrop spectrophotometer. Metagenomic libraries were prepared with the NEBNext Ultra DNA Library Prep Kit for Illumina (New England Biolabs Inc., USA) using around 200 ng of fragmented DNA as initial input. Size selection of 400–500 bp DNA library fragments was carried out using the Agencourt AMPure CP magnetic beads (Beckman Coulter Inc., USA) according to NEBNext Ultra DNA Library Prep Kit instructions. Each metagenomic DNA library was sequenced (100-nt paired-end sequencing) with the Illumina HiSeq.2500 platform using the TruSeq SR Cluster Kit, v3-cBot-HS (Illumina).

Raw 16S MiSeq paired reads were assembled and quality filtered with moira (Puente-Sánchez, Aguirre, & Parro, 2016) (v.1.3.2) with the -q posterior flag and then processed with mothur (Kozich et al., 2013; Schloss et al., 2011) to remove chimeras and sequences with poor alignments to the SILVA reference database (Pruesse et al., 2007; Quast et al., 2013). The pre-processed reads were analysed with CFF (Tikhonov et al., 2015) to achieve a subspecies resolution. The chimera-scanning step included in CFF's standard pipeline was omitted, as chimeras had already been removed with mothur's distribution of the VSEARCH software (Rognes et al., 2016). The resulting subspecies ESVs were classified with SINA (Pruesse et al., 2012) and also by homology search against the nt and 16S ribosomal RNA NCBI databases and the SILVA nr128 database distributed with mothur. Finally, any OTUs present in the BH10 samples that were also present in the drilling water control with an abundance of >0.5% of sample reads were discarded.

Generation of 454 amplicon libraries and community profiling

For pyrosequencing, the V3–V5 region of the 16S rRNA gene was amplified using key-tagged bacterial primers (ADM Lifesequencing, Spain) based on the design of Sim et al. (2012). PCR reactions were performed with 20 ng of metagenomic DNA, 200 µM of each of the four dNTPs, 400 nM of each primer, 2.5 U of FastStart HiFi Polymerase, buffer with MgCl₂

supplied by the manufacturer (Roche, Germany), 4% of 20 g/ml BSA (Sigma, UK), and 0.5 M Betaine (Sigma). TPCR cycling consisted of denaturation at 94°C for 2 min followed by 35 cycles at 94°C for 20 s, annealing at 50°C for 30 s, and extension at 72°C for 5 min. Amplicons were combined in a single tube in equimolar concentrations. The pooled amplicon mixture was purified twice (AMPure XP kit, Agencourt, UK) and requantified using the PicoGreen assay (Quant-iT, PicoGreen DNA assay, Invitrogen, Spain). EmPCR was performed and subsequently unidirectional pyrosequencing was carried out on a 454 Life Sciences GS FLX+ instrument (Roche, Germany) according to the Roche Amplicon Lib-L protocol. The resulting pyrosequencing reads were analysed as described by Schloss et al. (2011) and clustered at 3% distance with an average-neighbour algorithm. Any OTUs present in the BH10 samples that were also present in the drilling water control with an abundance of >0.5% of sample reads were discarded.

DNA extraction from the enrichment cultures

Approximately, 5–10 ml of the enrichment culture (containing both liquid medium and rock core particles) was pipetted out in the anaerobic chamber into a new 15 ml tube. After 30 min centrifugation at 4000 g, the supernatant was discarded and the pellet resuspended in 800 µl of phosphate buffer. The samples were then transferred to an empty Ultra-Clean Bead Tube and subjected to the same DNA isolation protocol described above. MDA amplification was not required for the enrichment culture DNA and thus we proceeded directly to the generation of MiSeq 16S rRNA amplicon libraries as described (Puente-Sánchez et al., 2018).

DNA extraction and 16S rRNA gene amplification, molecular cloning and sequencing

Total DNA was extracted from either 1 g of powdered cores or 1 ml of a suspension of powder in LifeGuard™ Soil Preservation Solution (MoBio Labs, USA) prepared less than 1 h after core sampling (1 g of powdered core + 5 ml of LifeGuard solution) and maintained at –20°C. The UltraClean® Soil DNA Isolation Kit (MoBio, USA) was used for DNA extraction, following manufacturer's instructions. The retrieved DNA was tested as a template for PCR amplification without any previous metagenome amplification. The universal bacterial primers for 16S rRNA gene used were: the forward 8F (5'-AGAGTTTGATCATGGCTCAG-3', positions 8–27 of *Escherichia coli* 16S rRNA) and either 1492R (5'-GGTTACCTTGTTACGACTT-3', positions 1510–1492)

or 16SR (5'-CACGAGCTGACGACAGCCG-3', positions 1089–1071) as the reverse ones. When required, nested PCR amplifications were performed, using the primer pairs 8F/1492R and 8F/16SR sequentially. In turn, the amplification of archaeal sequences using two archaeal-specific primer pairs: 21F (5'-TTAAGCTTGATCCTG CCGGA-3', positions 2–21, forward) and S (5'-GGTTACCTTGTTAC-GACTT-3', positions 1510–1492, reverse), or 20F (5'-TTCCGGTTGATCCYGCCRG-3', positions 2–20, forward) and U1392R (5'-ACGGGCGGTGTGTRC-3', positions 1392–1377, reverse) was attempted. Cloning amplified DNA fragments into *E. coli* and sequencing molecular clones was performed as previously described (Parro et al., 2011; Puente-Sánchez et al., 2018).

Fluorescence in situ hybridization

Chip rock samples were taken from the centre of the core as described (Escudero, Vera, et al., 2018).

Catalysed reported deposition fluorescence in situ hybridization

Samples were sonicated for three cycles of 20 s with one pulse per second at 20% intensity. The 100 µl of supernatant was filtered in 0.22-µm black membranes (Millipore, Germany) in aseptic conditions. Filters were washed with PBS and absolute ethanol and then air dried. Catalysed reported deposition fluorescence in situ hybridization (CARD-FISH) experiments were performed in membrane filters as previously described (Escudero, Vera, et al., 2018). The oligonucleotide probes for targeting rRNA genes used in this work are listed in Table S4. Stringencies were regulated for each probe by adjusting formamide (FA) and NaCl concentration in hybridization and washing buffer respectively (Table S4). Negative controls were performed with the NON338 probe (5'-ACTCCTACGGCAGGCGC-3'). Additional controls were carried out by subjecting the sample to the whole hybridization process without adding the probe, to evaluate whether the complex fluorophore-tyramide could interact with some minerals giving rise to false positives. No signal was obtained from these controls in multiple CARD-FISH experiments, and an additional inactivation of peroxidases was done between hybridizations.

FISH, DOPE-FISH and lectin binding assay and their respective controls

Rock samples were treated as described by Escudero, Vera, et al. (2018).

Ferric iron detection

Samples were stained with 2 µM Ferrum 430™ (Ursa BioScience, USA) diluted in ethanol/H₂O 90/10 (%v/v) for 10 min. Samples were washed with ethanol/H₂O 90/10 (v/v) and let air dry in darkness.

Counterstaining and mounting

Filters and rock samples were counterstained with 4',6-diamidino-2-phenylindole (DAPI) or Syto9 (Thermo Fisher Scientific, USA) as manufacturer recommended and covered with a mix of 1:4 Vectashield (Vector Laboratories, USA): Citifluor (Citifluor, UK). Filters were mounted onto glass slides and rock samples were mounted onto µ-slides eight-well glass bottom (Ibidi, Germany).

Confocal laser scanning microscopy

Subsurface samples were imaged in a confocal laser scanning microscope LSM710 coupled with an inverted microscope AxioObserver (Carl Zeiss, Germany) and equipped with diode (405 nm), argon (458/488/514 nm) and helium and neon (543 and 633 nm) lasers. Images were collected with a 63×/1.4 oil immersion lens. Images were processed using Fiji software (Schindelin et al., 2019).

FISH probe design

Probes were designed with the PROBE DESIGN tool from ARB software (Ludwig et al., 2004) as described in detail (Hugenoltz et al., 2002). S-G-Tess-681-a-A-21 (TESS681) and the competitor TESS681^c were designed to detect members of *Tessaracoccus* genus, S-S-Tlap-1449-a-A-18 (Tlap1449) for the detection of the species *Tessaracoccus lapidicaptus* and S-G-Rhi-124-a-S-22 (RHI124) to detect members of *Rhizobium* genus, in which are included the species *R. selenitirreducens* and *R. naphthalenivorans*. Designed probes were synthesized and labelled with CY3 fluorophore (Biomers, Germany). Specificity and optimal stringency conditions of the probes were determined in triplicate experiments. *Tessaracoccus lapidicaptus* IPBSL-7, *Tessaracoccus profundus* T2-5-50, *Rhizobium selenitirreducens* T2-30D-1.1 and *Rhizobium naphthalenivorans* T2-26MG-112.2, all isolated from enrichment cultures carried out in the IPBSL project (Leandro, 2018; Leandro et al., 2018; Puente-Sánchez, Sánchez-Román, et al., 2014), were used as positive hybridization control of the designed probes. *T. profundus* DSM21240, *T. oleiagri* DSM22955, *T. lubricantis* DSM19926, *T. flavescens* DSM18582,

used as additional positive controls for TESS681 probe, and *Deinococcus radiodurans* DSM20539, *Aeromicrobium ginsengisoli* DSM22238, *Rhizobium rosettiformans* DSM26376, which were used as negative controls for TESS681, Tlap1449 and RHI124, respectively, were purchased from the Leibniz Institute DSMZ-German Collection of Microorganisms and Cell Cultures (Braunschweig, Germany). All microorganisms were grown following DSMZ instructions. Optimal formamide concentration was determined at 50% for TESS681 probe, 10% for Tlap1449 probe and 50% for RHI124 probe.

Estimation of the number of cells per rock unit

Estimation of the number of cells per rock unit was performed by vortexing fixed powder and small rock chips at 4°C for 15 min in Sekar buffer (0.05% Tween80, 150 mM NaCl). Supernatant was filtered through membrane filters of 0.22 µm pore size (Millipore, USA) and washed with 1× PBS. Filters were embedded in 0.2% (w/v) agarose and subjected to CARD-FISH procedure as described previously using mixed EUB338 (I-III), ARC915, and NON338 probes (Table S4). Counts were performed manually with a fluorescence microscope Axioskop (Zeiss, Spain) in triplicate and at least 15 counting grids were counted per membrane section.

Activation of iron oxidation activity in rock samples by addition of anoxic sterile water

Powdered samples stored in anaerobic conditions from selected depths were placed into sterile 15 ml serum bottles under a N₂ atmosphere. As controls, subsamples from the same depths were sterilized at 120°C overnight and stored in the same conditions. Boiled milliQ water, gassed with N₂ during cooling was sterilized under N₂ atmosphere at 121°C for 20 min. The 5 ml of anoxic sterile milliQ water was added to the powdered rock containing bottles and incubated in darkness for 10 months at 37°C. Total iron concentration was monitored in duplicate by the α,α-dipyridyl method (Easton, 1972) with minimal modifications. Briefly, 10 µl of sample were mixed with 40 µl of hydroxylamine hydrochloride (10% in 1 M HCl), a reducing agent, and 100 µl of 40 mM sulfamic acid (in 1 M HCl). After 30 min, 150 µl of ammonium acetate (28%) was added to neutralize the pH to 5.5 and, after 5 min, 200 µl of α,α-dipyridyl (0.5% in absolute ethanol). Sterile 0.2 µm-filtered milliQ water was added until a final volume of 2 ml. Absorbance was measured at 520 nm with a U-2000 spectrophotometer (Hitachi, Japan). Ferrous iron concentration was determined without adding the hydroxylamine hydrochloride solution. Ferric iron

concentration was determined as the difference between total iron and ferrous iron concentrations.

Anaerobic iron oxidation by nitrate-reducing microorganisms

Acidovorax BoFeN1 (Kappler et al., 2005), *Shewanella* T2.3D-1.1, *Pseudomonas* T2.31.D-1 and *Tessaracoccus lapidicaptus* IPBSL-7 were grown in free-oxygen liquid media in triplicate. *Acidovorax* and *T. lapidicaptus* were grown in a basal media as described by Pantke et al. (2012). Basal medium was then amended with 10 mM NaNO₃ and 5 mM acetate for *Acidovorax* and 10 mM NaNO₃, 1 g/L glucose and 1 g/L yeast extract for *T. lapidicaptus*. The stock solutions of all of the compounds added to basal medium were autoclaved separately under N₂/CO₂ atmosphere for 20 min at 121°C, with exception of the vitamin solution, which was sterilized by filtration (0.2 µm). *Shewanella* T2.3D-1.1 and *Pseudomonas* T2.31.D-1 were grown in Luria-Bertani (LB) media autoclaved under N₂/CO₂ atmosphere (80:20) for 20 min at 121°C and amended with 10 mM NaNO₃. This media was used to grow the microorganisms in presence or absence of Fe²⁺. As a ferrous iron source, 4 mM FeCl₂ was added, dissolved in anoxic milliQ water and filtered as described by Easton (1972). The 15 ml of media were transferred into sterile 33 ml serum bottles that were closed with butyl rubber stoppers, crimped and flushed with N₂/CO₂ (80:20). Bottles were inoculated with 1 ml of *Acidovorax* BoFeN1, *Shewanella* T2.3D-1.1, *Pseudomonas* T2.31.D-1 or *T. lapidicaptus* IPBSL7 in exponential phase (~6 × 10⁶ microorganisms) which were grown in non-iron-containing medium. *Acidovorax*, *Shewanella* and *Pseudomonas* cultures were incubated at 28°C and *T. lapidicaptus* cultures at 37°C. Total iron, Fe²⁺ and Fe³⁺ concentrations were determined in duplicates as described above.

Scanning electron microscopy

Samples were analysed in a SEM-JEOL JSM-5600 LV apparatus (JEOL, Japan) complemented with an energy dispersive x-ray analyser (EDX). Rock samples were fixed in formaldehyde 5% in the field and were then processed following the procedure developed for observing rock-microorganism interactions (Shuster et al., 2019). This method includes the fixation of samples in glutaraldehyde and osmium tetroxide solutions, followed by dehydration in a graded ethanol series. Samples were mounted onto conductive graphite stubs and sputter and gold-coated in a Quorum Q150T-S apparatus (Quorum, United Kingdom) to ensure electrical conductivity and prevent charging under electron beams. Qualitative element compositions were

determined by Energy-Dispersive X-ray Spectroscopy (EDX) microanalysis using an INCAx-sight instrument with a Si-Li detector (Oxford, England) and a detection limit ca. 10% for major elements. Analyses were performed at room temperature using an accelerating voltage of 20 kV and working distance of 20 mm.

Occluded gases

Occluded H_2 , CO_2 and CH_4 in the rock samples were measured as follows: 27 ml vials were filled with chips and powder from selected samples leaving the minimal head space, under strict sterile and anoxic conditions in the anaerobic chamber. Vials were sealed with a gas-tight rubber septum and an aluminium cap, then flushed with N_2 . Incubations were static, in the absence of light, and done in a thermostatic chamber at $30 \pm 2^\circ C$. The gases that were released or consumed at different times (1, 4 and 8 months) were analysed using a gas chromatograph Bruker Series Bypass 450GC (Bruker, USA), equipped with a CP2056 $0.6\text{ m} \times 1/8''$ Ultimetel Cromsorb GHP 100-120 mesh and a CP81073 $0.5\text{ m} \times 1.8''$ Ultimetel Hayesep Q80-100 mesh columns with a thermal conductivity detector at $200^\circ C$ (for CO_2 and H_2) and flame ionization at $250^\circ C$ (for CH_4). N_2 was used as carrier gas.

Activated metabolism

The production of H_2 , CH_4 and CO_2 after the addition of enrichment culture mineral medium to powdered rock samples is considered a way to measure what we call the activated metabolism. To 0.5–1 g of powdered samples in 27 ml vials, sealed with butyl rubber septa and flushed with N_2 , 15 ml of mineral medium used for enrichment cultures (in g/L: 0.28 NH_4Cl , 0.33 $K_2HPO_4 \cdot 3H_2O$, 0.1 $MgSO_4 \cdot 7H_2O$, 2 $NaHCO_3$, 0.1 yeast extract and micronutrients as described by Sanz et al., 1997) were added. Incubations were static, in the absence of light, and done in a thermostatic chamber at $30 \pm 2^\circ C$. Gas generation was measured as described above at different times (1, 4 and 8 months).

Enrichment cultures

Enrichment cultures for the determination of different metabolic activities (methanogenic [MG], sulfate-reducing bacteria [SRB], denitrification [DNT], acetogenic [ACT] and methanotrophic [MT]) were carried out using 0.5–1 g of powdered rock samples from different depths in 130 ml serum bottles sealed with butyl rubber stoppers in sterile, dark and anaerobic conditions. Bottles were flushed with $N_2:CO_2$ 80:20 for 3 min. Incubations were static, in the absence of light, and done in a thermostatic chamber at $30 \pm 2^\circ C$. Controls were provided with the same mineral medium without substrate

added. For methanogenic, denitrification, acetogenic and methanotrophic activities, the following mineral medium was used in g/L: 0.28 NH_4Cl , 0.33 $K_2HPO_4 \cdot 3H_2O$, 0.1 $MgSO_4 \cdot 7H_2O$, 2 $NaHCO_3$, 0.1 yeast extract and micronutrients as described by Sanz et al., 1997. Cultures for methanogenic activity included, in addition to 50 ml of mineral medium, three different substrates: 2 mM acetate (MG1); $H_2:CO_2$ (80:20) in the head space (MG2) or a mixture of propionate + butyrate + methanol (5 mM each) (MG3). Methane production and H_2 and CO_2 consumption were measured with a gas chromatograph as described in the Subsection [Occluded gases](#). Cultures for autotrophic denitrification used 20 mM nitrate plus 20 mM thio-sulfate and $H_2:N_2$ (80:20) in 100 ml of mineral medium. Activity was measured as nitrate consumption by ion chromatography as described by Parro et al. (2011). For acetogenic activity, the substrates included a mixture of fumarate, propionate, butyrate, lactate, crotonate and ethanol (3 mM each) in 100 ml of mineral medium. Activity was measured by acetic acid production using an ion chromatograph as described by Parro et al. (2011). For methanotrophic activity, samples were incubated with CH_4 (99.999%) and 20 mM acetate in 50 ml of mineral medium. Activity was measured as CH_4 consumption by gas chromatography as described in the Subsection [Occluded gases](#). For sulfate reducing activities, 100 ml of basal medium SR was used containing in g/L: 0.53 $Na_2HPO_4 \cdot 2H_2O$; 0.41 KH_2PO_4 ; 0.3 NH_4Cl ; 0.11 $CaCl_2 \cdot 2H_2O$; 0.10 $MgCl_2 \cdot 6H_2O$; 0.3 $NaCl$; 4.0 $NaHCO_3$; 0.48 $Na_2S \cdot 9H_2O$; and micronutrients as described by Sanz et al. (1997). Sulfate reducing activities were assessed with 20 mM sulfate plus $H_2:N_2$ (80:20)/5 mM acetate (SRB1) or 20 mM sulfate plus lactate, methanol and glycerol (5 mM each) (SRB2). Sulfate reduction activity was measured as sulfate consumption using ion chromatography as described by Parro et al. (2011). Enrichment cultures for Fe oxidizers in anaerobic conditions were done as described in the Subsection [Anaerobic iron oxidation by nitrate-reducing microorganisms](#) for growth of *Acidovorax* and the activity measured as Fe^{3+} generation as described in the Subsection [Activation of iron oxidation activity in rock samples by addition of anoxic sterile water](#). Enrichment cultures for Fe reducers were done using the same mineral medium described above for denitrification, 10 mM glucose and 50 mM ferric sulfate. Activity was followed by the generation of Fe^{2+} and the consumption of Fe^{3+} in the conditions described in the Subsection [Activation of iron oxidation activity in rock samples by addition of anoxic sterile water](#).

Isolation of microorganisms from enrichment cultures

The most active methanogenic and nitrate-reducing enrichment cultures were used to obtain different

isolates in strict anaerobic conditions as described by Leandro (2018) and Leandro et al. (2018). Briefly, isolation of anaerobic microorganisms was performed by the Hungate roll-tube method (Hungate, 1969). Culture media for isolation of anaerobes had the same composition as the enrichment culture medium, including the addition of Agar Noble (15 g/L) (Difco) as solidifying agent. Hungate rolling tubes were inoculated with serial dilutions of each enrichment culture, respectively. Incubation was at 30°C in the dark until development of isolated colonies. Colonies were picked in anaerobic conditions with a bent Pasteur pipette and transferred into culture plates with the same cultivation conditions. Plates were incubated in anaerobic jars with Anaero-Gen sachets (Oxoid) to generate anaerobic conditions and in the case of cultures incubated with H₂:CO₂ (80:20, v/v), the gas mixture was injected inside the jar. Sub-culturing was done for at least two to three transfers. Colonies were screened for unique morphologies and representatives of each morphotype were selected for further identification.

Correlation analysis between most representative microorganisms and environmental variables

Excel 2013 was used for data collection. Statistical analyses were performed using R version 4.0.3. Data distribution was analyzed performing Shapiro–Wilk tests with the Shapiro test function included in the stats v4.0.3 package. Principal Component Analysis (PCA) was represented by the functions prcomp (included in the stat v4.0.3 package) and fviz_pcaplot to generate biplots (included in the FactoExtra v1.0.7 package). Data are represented in the plots by smaller dots and their geometric mean by large symbols.

Gene prediction analysis of sequenced subsurface microorganisms

The sequenced genomes of *Tessaracoccus lapidicaptus* IPBSL-7 (Puente-Sánchez, Pieper, & Arce-Rodríguez, 2016), *Tessaracoccus* sp. T2.5-30 (Leandro et al., 2017), *Brevundimonas* sp. T2.26MG-97 (Rodríguez-Robles et al., 2019), *Rhizobium* sp. T2.30D-1.1 (García et al., 2018), *Rhizobium* sp. T2.26MG-112.2, *Rhodoplanes* sp. T2.26MG-98 (Mariñán et al., 2019), *Pseudomonas* sp. T2.31D-1 (Martínez et al., 2020), *Shewanella* sp. T2.3D-1.1 (de Polanco et al., 2020) and *Desulfosporosinus merdii* DEEP, all of them isolated from the subsurface of the IPB, were used for gene prediction analysis and functional annotation. In addition, the IPB subsurface cyanobacteria sequences previously detected by shotgun metagenomics (Puente-Sánchez et al., 2018) were included in the analysis.

Gene prediction analysis and functional annotation was performed within the Integrated Microbial Genomes for *Tessaracoccus lapidicaptus* IPBSL-7 (IMG genome ID 2791354959), *Tessaracoccus* sp. T2.5-30 (IMG genome ID 2751185744) and *Desulfosporosinus merdii* DEEP (IMG genome ID 2721755100); with the NCBI annotation pipeline and PROKKA v1.12 software (Seemann, 2014) for *Brevundimonas* sp. T2.26MG-97 (NCBI accession number NZ_UXHF01000001.1), *Rhizobium* sp. T2.30D-1.1 (NCBI accession number NZ_UEYP01000001.1), *Rhizobium* sp. T2.26MG-112.2 (NCBI accession number NZ_UEYQ01000001.1), *Rhodoplanes* sp. T2.26MG-98 (NCBI accession number NZ_UWOC01000001.1), *Pseudomonas* sp. T2.31D-1 (ENA accession number CAJFAG01000000.1), *Shewanella* sp. T2.3D-1.1 (ENA accession CACVBT0200000010); and within the MG-RAST metagenomics analysis server for the Cyanobacteria (project ID mgp83581). Enzymatic activities of interest were defined based on the metabolic pathways described in the KEGG and MetaCyc databases (Caspi et al., 2014; Kanehisa & Susumu, 2000).

RESULTS

Drilling conditions, generation of samples and their physicochemical analysis

The selected drilling site was placed in the zone known as Peña de Hierro in the IPB (Gómez-Ortiz et al., 2014) (Figure S1). Borehole BH10, 613 m in depth, was continuously cored by rotary diamond-bit drilling, which produced 60 mm diameter cores protected by plastic liners and maintained under anoxic conditions. The retrieved cores were inspected visually in the drilling site and those selected for further analysis introduced in an anaerobic glove box, sectioned with a hydraulic guillotine at appropriate intervals, and the inner 20 mm ground out with a rotary hammer drill, under sterile and temperature-controlled conditions, to produce fine powdered samples for further analysis (for a detailed description see the [Experimental Procedures](#) section).

Mineralogical analysis of the cores revealed the presence of different minerals, with clinocllore (5.2% in 31.4% of the analysed samples), illite (4.6% in 40% of samples), pyrite (4.1% in 31.4% of samples), sericite (2.2% in 25.7% of samples), and siderite (1.5% in 13% of samples) being detected at higher concentration, all immersed in a quartz matrix (72.3% in 94.3% of the samples) (Dataset S1).

The elemental analysis of the core samples using ICP-MS showed a high concentration of metals, with the highest concentrations for Fe at 311.1, 206.6 and 139.4 metres below surface (mbs) with 129,234, 99,488 and 71,173 ppm, respectively, and Mn at 426.2, 414.0 and 450.3 mbs with 15,074, 10,442 and 2621 ppm, respectively. Interestingly enough, an elevated concentration of

Ti was detected along the length of the borehole, with the sample obtained at 487.0 mbs containing the highest concentration, 6761 ppm (Dataset S2).

The analysis of the water soluble cations showed the presence of NH_4^+ and oxidized and reduced Fe (Table S1). The highest concentrations of NH_4^+ were observed at 266.3, 450.3 and 130.8 mbs with 53.1, 46.4 and 43.9 ppm, respectively, and for soluble Fe at 311, 266.3 and 304.9 mbs with 705, 688 and 399 ppm, respectively. In general, Fe^{3+} concentrations were higher than Fe^{2+} , although some exceptions were observed (e.g. at 612.9 and 228.7 mbs).

To characterize the geochemical context, monitor any potential sample contamination from the drilling fluid and select samples for a microbial diversity analysis, rock leachates were routinely analysed *on site* by ion chromatography (IC). This allowed near real-time detection and quantification of the major water soluble inorganic and organic anions, including bromide (Br^-), which had been previously added to the drilling fluid as a contamination tracer (10 mg/L). Samples with a content of Br^- higher than 0.5 ppm were discarded from further analyses. Organic acids like acetate (highest concentrations at 336.5, 294.7 and 568.6 mbs with 200.6, 60.4 and 59.9 ppm, respectively), formate (highest concentrations at 460.0, 465.0 and 135.4 mbs with 6.7, 5.9 and 4.0 ppm, respectively), propionate (highest concentrations at 265.0, 475.3 and 580.2 mbs with 5.2, 3.5 and 2.7 ppm, respectively), and oxalate (highest concentrations at 450.3, 375.2 and 370.6 mbs with 6.5, 5.0 and 3.2 ppm, respectively), were detected along the borehole. The highest concentrations of phosphate were found at 135.4, 360.1 and 465.2 mbs with 10.2, 3.4 and 3.4 ppm, respectively. Sulfate was detected along the borehole with the highest concentrations at 310.3, 320.0 and 294.7 mbs with 634.5, 452.6 and 399.9 ppm, respectively. Nitrate was identified in most of the samples showing the highest concentrations at 375.2, 477.5 and 510.2 mbs with 2.5, 1.6 and 1.6 ppm, respectively, along with nitrite, the reduced product of nitrate, at 294.7, 295.0 and 320.0 mbs with 4.1, 3.4 and 2.8 ppm, respectively (Dataset S3).

Carbohydrates and proteins were also detected along the borehole. The highest concentrations of carbohydrates were obtained at 450.3, 498.8 and 266.3 mbs with 72.1, 43.0 and 39.2 ppm, respectively, and for proteins at 268.3, 519.1 and 492.6 mbs with 50.3, 40.0 and 33.1 ppm, respectively (Figure S2). The groundwater entering the ore body at Peña de Hierro was characterized by analysing upslope springs, and it was found to be aerobic, with neutral pH (7.4) and low conductivity (108 $\mu\text{S}/\text{cm}$).

Microbial diversity detection

Seven complementary methodologies: immunological detection, 16S rRNA gene sequencing, cloning,

hybridization (prokaryotic acidophilic microarray [PAM] and fluorescence in situ hybridization [FISH and CARD-FISH]), enrichment cultures and isolation, were used to identify the most representative microorganisms and their metabolic potential in 47 selected core samples.

Immunological detection

Twenty-one powdered core samples were analysed *on site* with the immunosensor Life Detector Chip (LDChip300) (Parro et al., 2011). The most abundant bacterial genera detected were *Shewanella* (12.4%), *Streptomyces* (10.6%), *Nostoc* (7.53%), *Acidithiobacillus* (7.5%), *Desulfosporosinus* (6.8%) and *Sulfobacillus* (5.6%). Members of the genus *Methanobacterium* (6.2%) were the only archaea identified along the column using this technique (Figure S3 and Table S2).

DNA analysis

DNA was recovered from 16 samples using various procedures (Table S3). Some of the DNA samples allowed us to obtain PCR amplicons of bacterial 16S rRNA genes directly, but most of them required prior isothermal amplification by multiple displacement amplification (MDA). Three amplified DNA samples were hybridized with a PAM (Garrido et al., 2008) with phylogenetic resolution (Figure S4 and Table S2). Amplified DNA samples were subjected to massive 16S rRNA gene ultra-deep sequencing (UDS) using two different techniques, Illumina MiSeq (12 samples) and Roche 454 (4 samples). Gpl (Cyanobacteria class) (19.9%), *Arthrobacter* (8.0%), *Acidovorax* (7.6%), *Tessaracoccus* (7.0%), *Bradirhizobium* (6.1%) and *Novosphyngobium* (6.0%) were the most abundant bacteria identified using Illumina MiSeq (Dataset S4 and Table S2). Gpl (Cyanobacteria class) (22.5%), *Aquabacterium* (20.7%), *Rhodoblastus* (12.7%), *Pseudomonas* (6.3%), *Bifidobacterium* (5.3%) and *Propionibacterium* (4.0%) were the most abundant bacteria identified using Roche 454 (Dataset S5 and Table S2).

Controls were performed to assess whether our samples could have been contaminated with the drilling fluid or during the subsequent analyses. As shown in the corresponding columns in Datasets S4 and S5, neither the water used as drilling fluid nor the internal control used during the manipulation of the samples gave important contamination values for the detected microorganisms in the different core samples. In any case, any OTU present in the BH10 samples that were also present in the drilling water control with an abundance >0.5% of sample reads was discarded.

To obtain more detailed taxonomic information, we retrieved nearly full 16S rRNA gene amplicons from nine core samples, which were then cloned and

sequenced (Dataset S6 and Table S2). The most abundant genera to which the identified species belonged were *Propionibacterium* (34.7%), Gpl (Cyanobacteria class) (12.5%), *Chroococcidiopsis* (6.9%), *Acidovorax* (5.6%), *Aquabacterium* (4.2%) and *Simplicispira* (4.2%).

However, despite several attempts, amplification of archaeal sequences using different sets of archaeal PCR primers and protocols were unsuccessful.

Fluorescence in situ hybridization

Scanning electron microscopy coupled to an energy dispersive x-ray probe (SEM–EDX) showed the presence of strong C signal microscopic structures, with sizes and morphologies typical of microorganisms, associated with mineral structures at different depths (Figure S5). To identify these microorganisms FISH and CARD-FISH were used (Escudero, Vera, et al., 2018). Positive hybridization signals using FISH were observed using different samples (Figure 1A,C,D). To improve resolution, a systematic analysis was performed with 35 selected samples using CARD-FISH with probes having complementary specificities (Table S4) to detect the presence of microorganisms along the column (Figures 2 and S6). The most-abundant identified bacteria corresponded to members

of the *Sulfobacillus* (14.5%), *Acidovorax* (13.2%), *Pseudomonas* (12.5%) *Rhodoplanes* (11.2%), *Tessaracoccus* (9.9%) and *Rhizobium* (7.2%) genera, while Methanosarcinales (7.8%) and Methanobacteriales (5.9%) were the most prevalent archaeal orders (Figure 2 and Table S2). Positive hybridization signals were detected using the anaerobic ammonium oxidation bacterial probe (ANAMMOX) (Figure S6E) at different depths (Figure 2) and the combination of the archaeal anaerobic methane oxidation (ANME 2) and SRB probes (Figure 1G). Co-occurrence of complementary microbial activities such as *Acidovorax*, an Fe oxidizer, and *Acidiphilium*, an Fe reducer (Figure 2), or *Sulfobacillus*, an S oxidizer, and SRBs (Figures 2 and S6N), were detected at different depths. Cell density along the borehole samples were estimated by hybridization of the extracted cells from the rock samples with Tween80 using a mixture of a bacterial and archaeal probes (EUB338 [I–III] and ARC915) yielding values between 10^4 and 10^5 cells/g of rock sample, regardless of depth.

Enrichment cultures and microbial isolation

To assess the metabolic potential of the microbial populations in the rock samples, anaerobic enrichment

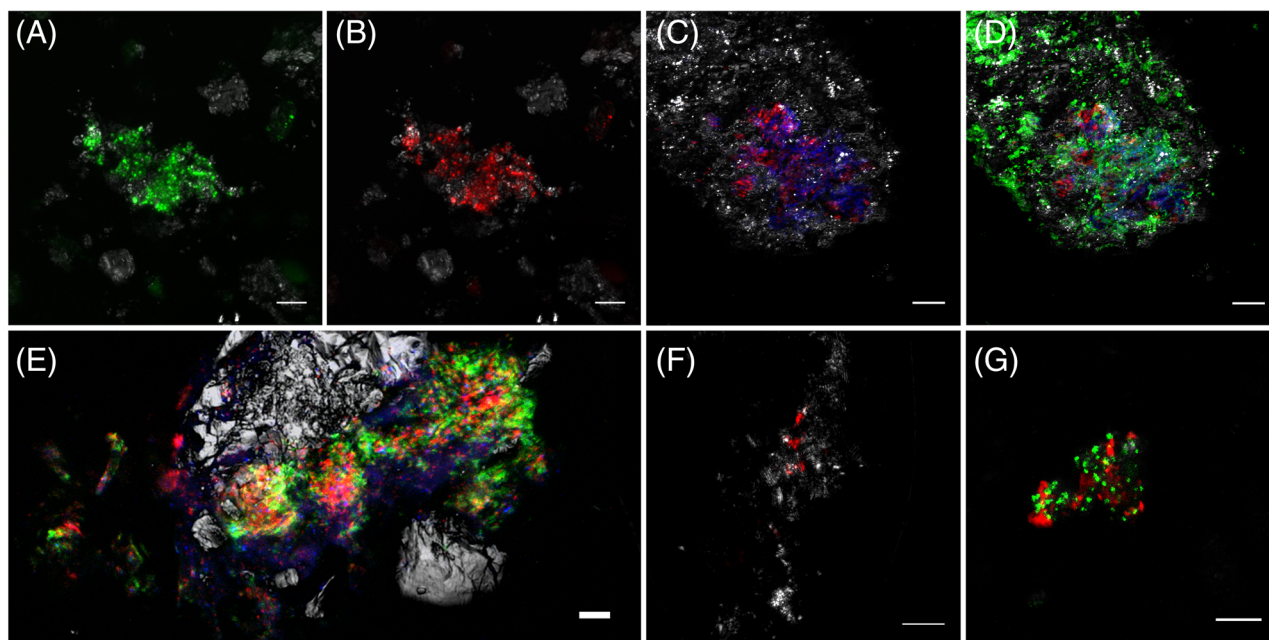


FIGURE 1 Active microorganisms, biofilms, microbial consortia and methanogenic activity detected by fluorescence in situ hybridization in the IPB deep subsurface. (A) and (B) FISH detection of Archaea (red) at 414 mbs using probe ARC915 and differential staining with Syto9 (green); (C) DOPE-FISH detection of a mixed biofilm of Bacteria (red) and Archaea (blue) at 139.4 mbs using EU 338 (I–III), ARC915 probes and FLBA with ConA, AAL and PNA lectins (green); (D) same as (C) after FLBA signal filtration. CARD-FISH detection: (E) co-occurrence of an Fe oxidizing bacteria *Acidovorax* (red, probe ACI145), an iron reducer *Acidiphilium* (yellow, probe ACD840), a S oxidizer *Sulfobacillus* (blue, probe SUL228), and S reducing bacteria (green, probe SBR385); (F) methanogenesis at 355.7 mbs by members of the order Metanobacteriales (probe MEB859); (G) anaerobic oxidation of methane at 206.6 mbs promoted by the interaction of members of the *Desulfosarcina-Desulfococcus* genera (red, probe DSS658) with members of the ANME 2 archaeal group (green, probe ANME-2-538). In grey, reflection. Scale bars 5 µm with the exception of (C) and (D): 10 µm

IPBSL-BH10

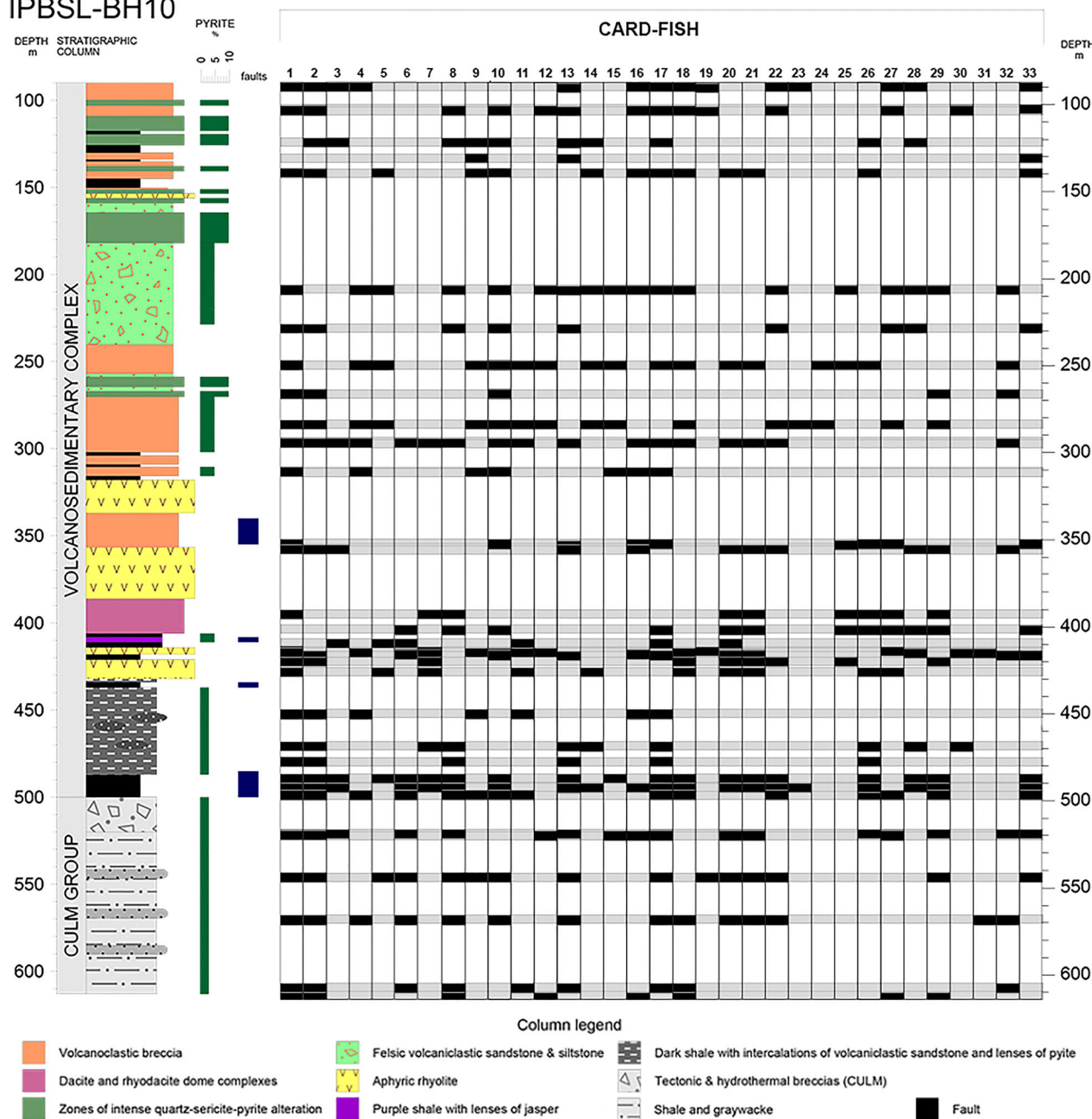


FIGURE 2 Mineralogy and microbial diversity detected by CARD-FISH along the BH10 borehole. Hybridization probes, described in Table S4, with the following specificities were used for microbial detection: 1: Bacteria (I-III); 2: Planctomycetales; 3: ANAMMOX, 4: α -Proteobacteria; 5: *Acidiphilium* spp.; 6: *Rhizobium* spp.; 7: *Brevundimonas* spp.; 8: *Rhodoplanes* spp.; 9: β -Proteobacteria; 10: *Acidovorax* spp. (I and II); 11: γ -Proteobacteria; 12: *Acidithiobacillus* spp. (I and II); 13: *Pseudomonas* spp.; 14: SRB/ δ -Proteobacteria; 15: *Desulfosarcinal Desulfococcus*; 16: Firmicutes (a and b); 17: *Sulfobacillus* spp.; 18: Actinobacteria; 19: *Propionibacterium* spp.; 20: *Tessaracoccus* spp.; 21: *T. lapidicaptus*; 22: Acidobacteria; 23: Bacteroidetes; 24: *Leptospirillum* spp.; 25: Cyanobacteria; 26: Chloroflexi (I and II); 27: Archaea; 28: Euryarchaeota; 29: Methanosarcinales; 30: Methanococcaceae; 31: Methanomicrobiales; 32: Methanobacteriales; 33: Crenarchaeota. In black, positive hybridization signals; in grey, negative hybridization signals

cultures in diverse media, containing selected electron donors and acceptors, were set up within 24 h after generation of the core samples. Iron oxidation (highest activity detected at 336.5 mbs), iron reduction (highest activity at 413.3 mbs), sulfate reduction (highest activity at 352.7 mbs), methanogenesis (highest activity at 228.7 mbs), methanotrophy (highest activity at

352.7 mbs), acetogenesis (highest activities at 433.3 mbs) and autotrophic denitrification (highest activity at 352.7 mbs), were detected along the entire borehole (Table S5). Co-occurrence of complementary metabolic reactions such as Fe oxidation and reduction were detected in samples from the same depth (at 311.1, 336.5, 352.7, 353.2, 393, 414 and 568 mbs).

The microbial composition of the nine most active enrichment cultures (acetogenesis at 304.9, 311.1, 355.7, 414 and 433.3 mbs; sulfate reduction at 284, 520 and 568.6 mbs; and methanogenesis at 228.7 mbs) was determined using Illumina MiSeq. The most-abundant microbes in these cultures belonged to the *Tessaracoccus* (30.3%), *Pseudomonas* (27.5%), *Propionibacterium* (12.6%), *Desulfurispora* (12.5%), *Desulfobibrio* (6.2%), *Acetobacterium* (4.2%) and *Rhodoplanes* (3.8%) (Dataset S7).

Twenty-nine microorganisms were isolated from the most active methanogenic and autotrophic denitrification enrichment cultures under strict anaerobic conditions (Leandro, 2018; Leandro et al., 2018). Microorganisms identified as members of the genera *Acetoanaerobium*, *Aestuarimicrobium*, *Bacillus*, *Brevundimonas*, *Cellulomonas* (two isolates), *Desulfovibrio*, *Lelliotia*, *Macellibacteroides*, *Microbacterium*, *Nocardoides*, *Paenibacillus*, *Propionimonas*, *Pseudomonas* (five isolates), *Rhizobium* (two isolates), *Rhodoplanes* (three isolates), *Shewanella*, *Tessaracoccus* (four isolates) and *Xanthobacter* were isolated in the conditions described in Supplementary Material section (Table S6).

Occluded gases and their evolution after induction

Since the identified potential metabolic activities either produce or consume various types of gases, occluded H₂, CO₂ and CH₄ were measured by gas chromatography (GC) in the retrieved samples. The highest concentration for H₂ was observed at 121.8 mbs, for CO₂ at 487.2 mbs, and for CH₄ at 353.2 mbs (Table S7). In addition, the evolution of these gases was observed after mineral media was added (activated metabolism). In general, metabolic activation resulted in an increase in the release of these gases, at 284 and 409.7 mbs for H₂, at 266.3 and 352.7 mbs for CO₂, and 414 mbs for CH₄. Consumption of these gases was also observed, for example, at 336.5 mbs for H₂, 487.2 mbs for CO₂, and 353.2 mbs for CH₄ (Table S7).

Identification of the most representative genera

Based on detection by 2 or more independent methodologies at a minimum of 5 depth intervals of the 19 analysed, the most representative genera along the borehole were selected. Using these criteria 1 class, Cyanobacteria, and 16 genera, *Acidiphilium*, *Acidovorax*, *Acidithiobacillus*, *Arthrobacter*, *Bacillus*, *Brevundimonas*, *Desulfosporosinus*, *Desulfovibrio*, *Leptospirillum*, *Propionibacterium*, *Pseudomonas*, *Rhizobium*, *Rhodoplanes*, *Shewanella*, *Sulfobacillus* and *Tessaracoccus*, were selected and submitted to a more in-depth analysis (Figure 3, Table S2). The most representative genera

were *Pseudomonas* (12.6%), *Tessaracoccus* (10.8%), *Sulfobacillus* (10.5%), *Acidovorax* (7.5%), *Desulfosporosinus* (7.5%), and *Rhodoplanes* (7.2%) together with members of the Cyanobacteria class (7.5%).

Correlations between the most representative genera and different environmental variables

Five genera, *Acidovorax*, *Arthrobacter*, *Pseudomonas*, *Rhodoplanes* and *Sulfobacillus*, showed a positive correlation with Fe content and pyrite; *Acidiphilium* and *Tessaracoccus* showed a correlation with Cu and clinocllore; *Brevundimonas* with Zn and illite, *Shewanella* with siderite; *Bacillus* with Mn and Cyanobacteria with pyrite (Figure 4). No correlations were observed between the most representative microorganisms and gases or identified metabolisms.

Genomic analysis of isolated microorganisms

The sequenced genomes of nine IPB subsurface isolates belonging to *Brevundimonas* (Rodríguez-Robles et al., 2019), *Desulfosporosinus* (this work), *Pseudomonas* (Martínez et al., 2020), *Rhizobium* (two isolates, García et al., 2018 and this work), *Rhodoplanes* (Mariñán et al., 2019), *Shewanella* (de Polanco et al., 2020) and *Tessaracoccus* (two isolates, Leandro et al., 2017; Puente-Sánchez, Pieper, & Arce-Rodríguez, 2016) genera, and the sequences obtained by shotgun metagenomics of the Cyanobacteria detected in BH-10 (Puente-Sánchez et al., 2018), all of them selected as representative bacteria of the ecosystem, were annotated to identify the presence of genes involved in different metabolic activities (Figure 5, Table S8 and Dataset S8). The complete set of genes coding for the enzymatic activities required to functionally maintain the complete C, H, N, S and Fe cycles were annotated at eight different depths (392, 414, 477.5, 487.2, 496.8, 544, 568.6 and 607 mbs). The genes involved in the generation of CO₂ were present in 75.9% of the identified microorganisms; for N₂ fixation, H₂ oxidation and complete denitrification in 39.3%; for nitrate reduction to nitrite, dissimilatory nitrate reduction to ammonium (DNRA) and sulfur oxidation in 35.7%; for CO₂ fixation in 25%; for sulfur reduction in 23.2%; and for Fe reduction and H₂ generation by fermentation in 14.3% (Figure 5 and Table S8).

Fe oxidation coupled to nitrate reduction activity

The addition of oxygen-free sterile milliQ water to three dry core samples selected for their pyrite content and

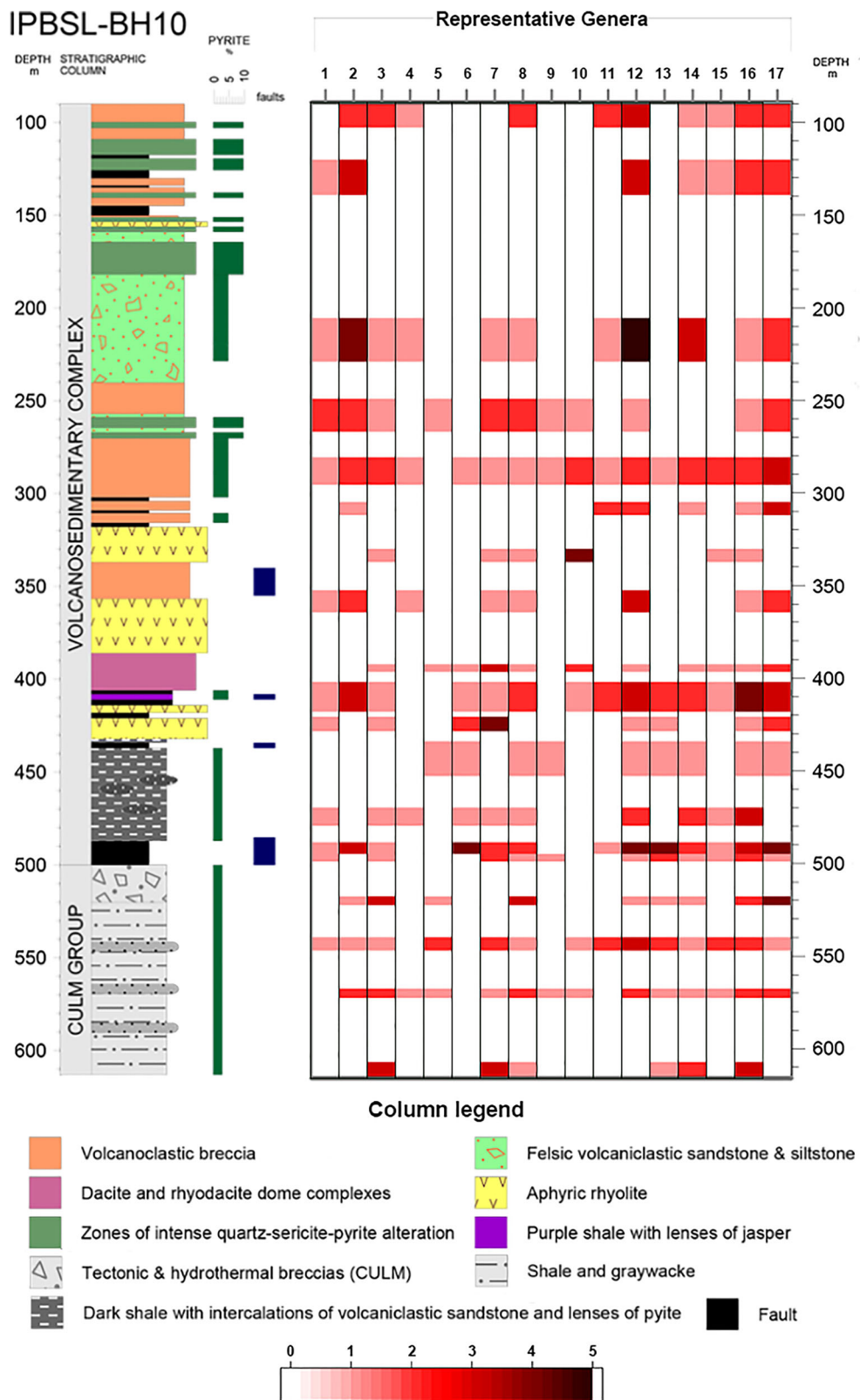


FIGURE 3 Most representative microbial genera identified in the deep subsurface of the IPB. Genera detected by two or more independent methodologies at least at five depths intervals along the borehole BH10 are displayed. Hot tones correspond to the number that a given genus has been detected in a depth interval. 1: *Acidiphilium*, 2: *Acidovorax*, 3: *Acidithiobacillus*, 4: *Arthrobacter*, 5: *Bacillus*, 6: *Brevundimonas*, 7: *Cyanobacteria*, 8: *Desulfosporosinus*, 9: *Desulfovibrio*, 10: *Leptospirillum*, 11: *Propionibacterium*, 12: *Pseudomonas*, 13: *Rhizobium*, 14: *Rhodoplanes*, 15: *Shewanella*, 16: *Sulfobacillus*, 17: *Tessaracoccus*

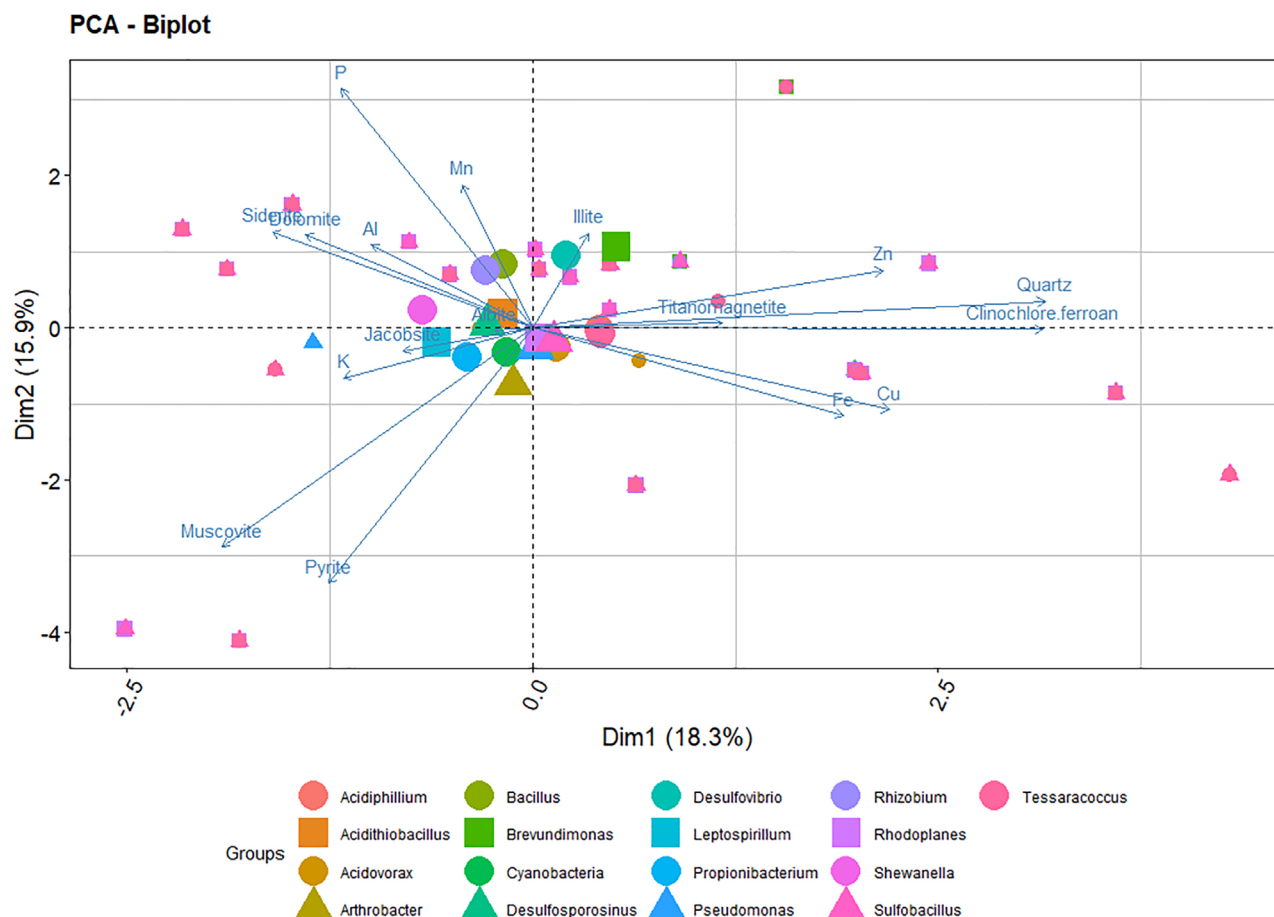


FIGURE 4 Principle component analysis of the selected representative microorganisms and the mineralogical and geochemical parameters along the borehole. Data are represented in the plots by small dots and their geometric mean represented by large dots.

maintained under anaerobic conditions (samples from 102.6, 139.4 and 228.6 mbs with 10.6%, 8.3% and 8.5% of pyrite, respectively), generated visible ferric iron, which was not observed in previously sterilized samples. The correspondent soluble Fe content measured after 10 months incubations was 4.6, 6.2 and 0.24 g/L, respectively (Figure S7). To verify that iron oxidation was biologically mediated, four nitrate-reducing bacteria identified as representative in the IPB subsurface, *Pseudomonas* sp. T2.26MG-48.2, *Shewanella* sp. T2.3D-1.1 and *Tessaracoccus* sp. T2.5-30, all IPB isolates (Table S6), and *Acidovorax* BoFeN1 (used due to the lack of an available *Acidovorax* IPB isolate), were incubated in the presence of Fe^{2+} and were able to oxidize reduced Fe with different efficiencies after 20 days of incubation in strict anaerobic conditions when compared with the oxidation produced by *Acidovorax* (100% for *Pseudomonas*, 98% for *Shewanella*, and 43% for *Tessaracoccus*) (Table S9). This Fe oxidizing activity could be also visualized in situ by fluorescence microscopy (as shown at 418 mbs for *Acidovorax* and at 228.6 mbs for *Tessaracoccus*) (Figure S8).

DISCUSSION

Continental deep subsurface geomicrobiology is essential to our understanding of the importance of Earth's biogeochemical cycles at a local and planetary scale. Recent evaluations estimate that most of the prokaryotic biomass is located in the deep subsurface (Colman et al., 2017; Magnabosco et al., 2018). Unfortunately, most of the available subsurface continental microbiological information has been obtained from groundwater samples, with their intrinsic limitations (Escudero & Amils, 2022; Escudero, Oggerin, & Amils, 2018). To generate information on the abundance, diversity, as well as microbiome functions in continental subsurface rock systems, devoted drillings are required to generate core samples with which to perform essential complementary analysis. The few devoted continental drilling operations carried out to date have reported, in general, microbial diversity information from samples obtained at great depth distances and/or using just one methodology, which do not produce sufficient reliable information to describe the operation of the biogeochemical cycles in the deep subsurface (Breuker et al., 2011;

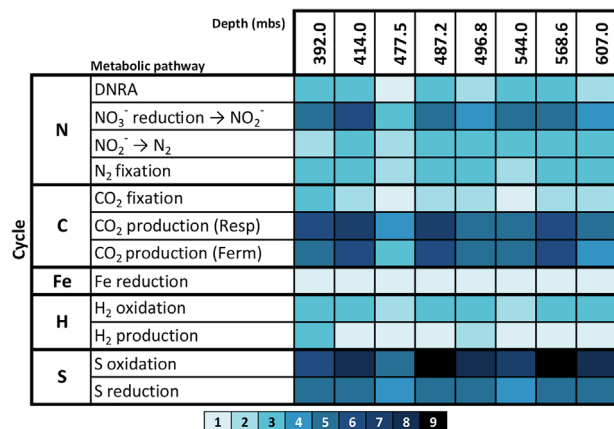


FIGURE 5 Genetic potential for the operation of complete biogeochemical cycles along borehole BH10. Genomic information from nine subsurface IPB isolates: *Brevundimonas* sp. T2.26MG-97, *Desulfosporosinus meridei* DEEP, *Pseudomonas* sp. T2.31D.1, *Rhizobium* sp. T2.30D-1.1, *Rhizobium* sp. T2.26MG-112.2, *Rhodoplanes* sp. T2.26MG-98, *Shewanella* sp. T2.3D-1.1, *Tessaracoccus* sp. T2.5-30, *Tessaracoccus lepidicaptus* IPBSL-7 and shogun metagenomic data for Cyanobacteria, all of them identified as most representative bacterial genera in borehole BH10 (Figure 3) were used to identify the genes responsible for the functional operation of C, H, N, S and Fe cycles at different depths. Hot tones correspond to the number of microorganisms in which the complete set of genes coding for the enzymes required for a given activity have been detected at a given depth. DNRA, dissimilatory nitrate reduction to ammonium. Only samples with potential to complete all five cycles are displayed.

Cockell et al., 2021; Dutta et al., 2018; Fry et al., 2009; Lehman et al., 2004; Liu et al., 2020; Momper, Reese, et al., 2017; Zhang et al., 2005). To overcome these limitations, this work employed 47 core samples, in order to generate an exhaustive complementary and multidisciplinary analysis of the microbiology and microbial-driven geochemical processes operating in the deep subsurface of the IPB.

The Iberian Pyrite Belt Subsurface Life Detection project (IPBSL) was planned to evaluate the existence of an underground reactor as the possible origin of the extreme conditions detected in the Río Tinto basin. A thorough geophysical analysis using resistivity tomography (ERT) and time-domain electromagnetic sounding (TDEM) allowed the subsurface areas where water and reduced minerals were most likely to intersect to be identified, producing representative information on the mineral substrates and the associated microbial diversity that exists in the deep subsurface of the IPB (Gómez-Ortiz et al., 2014). The selected drilling site, BH10, is located on the north flank of the Río Tinto anticline, in the area known as Peña de Hierro (Iron Mountain) (Figure S1). Borehole BH10 was drilled through the upper part of the volcano sedimentary complex of the district, which hosts a large zone of hydrothermal alteration with widespread replacement by quartz, clinohlore, illite, pyrite, sericite and siderite. Among these

minerals, most contained Fe, which agrees with the elemental content detected by ICP-MS along the borehole (Datasets S1 and S2).

From our previous drilling experience, we had learned that a fast in situ geochemical analysis of the retrieved cores was the best way to select samples for a deeper analysis (Fernández-Remolar et al., 2008; Puente-Sánchez, Moreno-Paz, et al., 2014). The use of IC *on site* to analyse the soluble anionic content of core samples overnight allowed samples with an interesting pattern of electron acceptors, content of organic acids and with low levels of Br[−] (used as a drilling fluid contamination marker) to be selected. From among the different contamination markers tested in previous drilling operations in the IPB (Amils et al., 2008; Fernández-Remolar et al., 2008; Puente-Sánchez, Moreno-Paz, et al., 2014) Br[−] was selected due its low concentration in the subsurface of the IPB, its efficient detection with IC, economical price and ecological considerations. The presence of organic acids such as acetate, formate, oxalate and propionate identified at different depths is good indicator of the presence of biological activity along the column. Of these, acetate and formate are interesting metabolic products, which can be used as electron donors and a source of carbon for other subsurface microorganisms (Purkamo et al., 2017). The detection of sulfate strongly suggests the existence of active bioleaching of metal sulfides along the borehole (Vera et al., 2013) and the existence of SRB (Bell et al., 2020; Itävaara et al., 2011; Momper, Jungbluth, et al., 2017; Onstott et al., 2009). The presence of nitrate, nitrite and ammonia are good indicators of an operative nitrogen cycle (Lau et al., 2014; Rempfert et al., 2017). All these data together with the detection of carbohydrates and proteins at different depths were strong signals of the existence of extant or recent microbiological activities in the subsurface of the IPB (Dataset S3).

To overcome the bias introduced using only one methodology to describe microbial diversity along the borehole and the problems associated with the unavoidable contamination associated with drilling operations (Sheik et al., 2018), complementary methodologies based on different principles (immunological, sequencing, cloning, hybridization, enrichment cultures and isolation) were used to identify, at the genus level, the most representative microorganisms along the borehole.

Although extracting high-quality nucleic acids from hard rock cores is always challenging, we were able to recover DNA from 16 core samples from different depths to identify the bacterial diversity along borehole BH10. PCR amplicons from these samples were analysed through hybridization with PAM (Garrido et al., 2008), cloning and massive 16S rRNA gene ultra-deep sequencing by means of two techniques, Illumina MiSeq and Roche 454. Despite the use of

several recommended sets of archaeal PCR primers and diverse protocols, we were unable to amplify 16S rDNA sequences for Archaea, although we know that members of this domain are present in the deep subsurface of the IPB because other methodologies, like immunological (LDchip300) and hybridization (FISH and CARD-FISH), gave positive identification results. It seems that insufficient yield in the preparation of DNA and/or the integrity of 16S rDNA contained in the retrieved samples are the most plausible causes for this unfortunate situation. Of the different methodologies used in this work, FISH and CARD-FISH stands out because it not only identifies the presence of microorganisms but also quantifies them and detects their close contact with other microorganisms, suggesting the functional operation of complementary metabolic activities. In this work, we have detected the presence of ANAMMOX bacteria, which could be responsible for the oxidation of the NH_4^+ detected in the column (Kuenen, 2008; Strous et al., 2006); the co-occurrence of archaeal ANME-2 and SRB, which could explain the methanotrophic activities detected along the borehole (Knittel & Boetius, 2009); the co-occurrence of the Fe oxidizer *Acidovorax* and the Fe reducer *Acidiphilium* suggesting the operation of an Fe cycle (Kappler et al., 2021) and the sulfur oxidizer *Sulfobacillus* and SRB suggesting the operation of an S cycle (Bell et al., 2020) (Figures 1 and 2). To the best of our knowledge, this is the first time that anaerobic ammonia oxidation and methanotrophy have been identified using FISH in continental hard rock samples from the deep subsurface. In addition, an important advantage over the rest of the methodologies used is that FISH requires only a very small sample, generating information on the presence of different microorganisms at microscopy size resolution, which is unobtained with the rest of the methodologies employed as they require larger quantities of sample for their analysis. In the case of solid rock matrices a fair amount of sample is required to obtain analysable DNA, in our case between 0.5 and 10 g of core samples. Furthermore, FISH is a non-destructive method that allows the same sample to be re-hybridized using complementary probes. This facilitates the identification of the diverse microbial components of the sample. Except for FISH, the other methodologies yield interesting diversity results but without information on the interconnection between the identified microorganisms and the mineral features of the complex matrix in which they inhabit.

The positive hybridization signals using the FISH protocol strongly suggest the presence of metabolically active microorganisms in the deep subsurface (Figure 1), a fundamental question in subsurface geomicrobiology (D'Hondt et al., 2002; Escudero, Oggerin, & Amils, 2018; Lovley & Chapelle, 1995; Morita, 1999; Phelps et al., 1994). In this work, most of the microbial identification has been done using CARD-

FISH to amplify the hybridization signal and facilitate the distinction between real hybridizations and artefacts, such as unspecific binding of the probe or the dye (Escudero, Vera, et al., 2018). In addition, FISH demonstrated the existence of biofilms in the oligotrophic deep subsurface of the IPB (Figure 1), contrary to the generally accepted idea that in these conditions microorganisms are unable to use their limited source of energy in the generation of very metabolically expensive structures (Escudero, Vera, et al., 2018; Poulsen et al., 1993; Sauer, 2003; Saville et al., 2011). From our data, we strongly support the idea that if needed microorganisms will use their limited resources to make biofilms, to take advantage of their useful properties such as the ability to interconnect metabolically complementary functional microorganisms, protect against desiccation, control metabolic products diffusion, and so on (Coyte et al., 2017; Vera et al., 2013).

As observed at other continental drilling operations in the subsurface of the IPB Bacteria are much more abundant than Archaea (Figure 2) (Breuker et al., 2011; Dutta et al., 2018; Fry et al., 2009; Magnabosco et al., 2018; Momper, Reese, et al., 2017; Suzuki et al., 2013; Takai et al., 2001; Zhang et al., 2005), which seems to be a common property of the continental deep subsurface. We did not observe any depth-related patterns of distribution of taxonomic/functional groups along the column, at least along the 612 m analysed. Despite the difficulties in assessing cell density within a solid, low-porosity rock and variable mineralogical content, conservative estimates derived from the analysis of different samples along the borehole yielded values between 10^4 and 10^5 cells/g of rock sample, regardless of depth. This is in the same order of magnitude as that reported for other continental hard rock drilling operations (Breuker et al., 2011; Cockell et al., 2012; Cockell et al., 2021; Dutta et al., 2018; Fry et al., 2009; Onstott et al., 2003).

A convenient system to identify putative microbial metabolisms in the deep subsurface is to establish enrichment cultures for suspected activities related with the detected geochemical variables. Obviously, enrichment cultures have the bias that the conditions are optimal for the observation of those activities selected and these can be quite different from those existing in the native subsurface conditions, giving opportunistic microbes the advantage over the rest of the microorganisms. In our case, enrichment cultures were used to test the metabolic activities, which were expected due to the characteristics of the ecosystem, such as iron and sulfide oxidation (Fernández-Remolar et al., 2008). Other activities, for example, methanogenesis and sulfate reduction were selected because they had been detected on previous drilling campaigns in the IPB (Puente-Sánchez, Moreno-Paz, et al., 2014). And finally, activities related with the detected geochemical compounds along the borehole, like acetogenesis

(acetate), methanotrophy (CH_4) and nitrate-reducing activities (NO_3^-) were also selected.

Although we could not generate archaeal sequences in this work, the presence of methanogenic archaeal activity was confirmed using complementary methodologies. The presence of occluded CH_4 in different samples and CH_4 produced after core samples activation, together with the presence of H_2 and CO_2 , the substrates for hydrogenotrophic methanogenesis, are strong indicators for the existence of methanogenic activities in the ecosystem. Recently, it has been shown that an important proportion of H_2 and CO_2 detected in the subsurface of the IPB are biologically produced (Mateos et al., 2022; Sanz et al., 2021). This observation is extremely important in our ecosystem because it is generally assumed that most of the detected H_2 in the subsurface is abiotically produced (Pedersen, 1997; Stevens & McKinley, 1995). The generation of CH_4 was detected, with variable intensities, along the length of the borehole, using hydrogenotrophic, acetoclastic and methylotrophic substrates (Table S7). These results agree with the detection of *Methanobacterium* using the immunological LDChip300 and the positive hybridization signals observed using specific hybridization probes for Methanosarcinales and Methanobacteriales orders (Figures 1F and 2). Methanogenesis was one of the first activities detected in the continental deep subsurface and has been reported in most of the drilling operations (Kotelnikova, 2002; Pedersen & Albinsson, 1992).

The presence of CH_4 along the column called for testing for the presence of methanotrophic activities. Methanotrophy was detected at variable intensities in diverse enrichment cultures from core samples at different depths (Table S7). As in other anoxic environments, this activity requires the syntrophic cooperation of an archaeal anaerobic methane oxidizer (ANME 2) and a SRB. This co-occurrence was observed using specific hybridization probes for both types of microorganisms (Figure 1G). Although ANME archaea (Fry et al., 2009) and SRB (Motamedi & Pedersen, 1998) have been identified previously in the continental deep subsurface; to the best of our knowledge, this is the first demonstration of this syntrophic activity in the hard rock matrix of a deep subsurface. Knowing that this activity can also be obtained by syntrophic association of ANME 2 archaea with nitrate and iron-reducing activities, and that both activities occur in the subsurface of the IPB (Table S5), it is reasonable to expect anaerobic oxidation of methane through these activities in the subsurface of the IPB (Schnakenberg et al., 2021).

Five additional activities have been detected using enrichment cultures: acetogenesis, autotrophic denitrification, Fe oxidation, and sulfate and Fe reduction. As shown in Table S5, these activities were detected in core samples at different depths with variable intensities as expected for an irregular solid matrix.

Acetogenic activity, also described previously in the continental deep subsurface (Magnabosco et al., 2016; Rempfert et al., 2017), could be predicted by the high concentration of acetate detected along the column. Autotrophic denitrification was considered an activity of interest after the detection of nitrate and nitrite by IC and the presence of reduced sulfur compounds generated by the operation of the S cycle (Lau et al., 2016). Sulfate-reducing activity (SRB) was also expected due to the presence of SO_4^{2-} as a result of the metal sulfides oxidation. Sulfate-reducing activity is also a classical metabolic activity detected in continental deep subsurface (Motamedi & Pedersen, 1998; Onstott et al., 2009). In the case of SRB, two electron donors were used, H_2 and a mixture of lactate, methanol and glycerol. The generation of H_2S from the sulfate-reducing activity can explain the detection of secondary pyrite and the attack of primary sulfates under reducing conditions (e.g. baryte, BaSO_4) through the biological activity along the borehole (Fernández-Remolar et al., 2008, 2018). The highest activities detected for sulfate reduction, methanotrophy and autotrophic denitrification at 352.7 mbs could be related to the presence at this depth of a fault, which facilitates the water and dissolved substrates movement.

Enrichment cultures for anaerobic Fe oxidation and Fe reduction activities were tested with core samples along the column (Table S5). In the case of anaerobic Fe oxidation, acetate was used as electron donor and nitrate as electron acceptor, both compounds detected in the IPB subsurface. For Fe reduction, glucose was used as electron donor. Table S5 shows the distribution of both activities along the borehole. The detection of both activities at the same depth in 8 out of the 32 analysed samples, suggest an operative Fe cycle in the subsurface of the IPB, which agrees with the co-occurrence of Fe oxidizing and reducing microorganisms observed by hybridization (Figures 1, 2 and S6).

Sixteen genera belonging to the Pseudomonadota (*Acidiphilium*, *Acidovorax*, *Acidithiobacillus*, *Brevundimonas*, *Desulfovibrio*, *Pseudomonas*, *Rhizobium*, *Rhodoplanes*, *Shewanella*), Actinomycetota (*Arthrobacter*, *Propionibacterium*, *Tesaraococcus*), Bacillota (*Bacillus*, *Desulfosporosinus*, *Sulfobacillus*) and Nitrospirata (*Leptospirillum*) phyla and members of the class Cyanobacteria, were selected as the most representative bacterial genera in the subsurface of the IPB as they were detected by at least two independent methodologies at five depth intervals (Figure 3).

Pseudomonadota, Actinomycetota and Bacillota have been described as the most common phyla identified in the continental deep-subsurface (Fry et al., 2009; Magnabosco et al., 2016; Nuppunen-Puputti et al., 2022; Onstott et al., 2009; Wu et al., 2016; Zhang et al., 2005). Members of the most representative genera were previously identified in different continental deep subsurface drilling operations,

Acidiphilium (Cockell et al., 2021; Johnson, 2012), *Acidovorax* (Liu et al., 2020; Miyoshi et al., 2005; Onstott et al., 2003; Shimizu et al., 2006), *Acidithiobacillus* (Johnson, 2012; Lau et al., 2016), *Brevundimonas* (Bell et al., 2020; Bose et al., 2020; Nuppenen-Puputti et al., 2022; Onstott et al., 2009), *Desulfovibrio* (Bell et al., 2020; Motamedi & Pedersen, 1998; Shimizu et al., 2006), *Pseudomonas* (Boivin-Jahns et al., 1996; Onstott et al., 2009; Shimizu et al., 2006; Zhang et al., 2005), *Rhizobium* (Dutta et al., 2018; Momper, Reese, et al., 2017; Zhang et al., 2005), *Shewanella* (Dutta et al., 2018; Fredrickson et al., 1998; Onstott et al., 2009), *Arthrobacter* (Lehman et al., 2004; Zhang et al., 2005), *Propionibacterium* (Boivin-Jahns et al., 1996), *Tessaracoccus* (Cockell et al., 2012), *Bacillus* (Cockell et al., 2012; Dutta et al., 2018; Onstott et al., 2009; Zhang et al., 2005), *Desulfosporosinus* (Onstott et al., 2009), *Sulfobacillus* (Gihring et al., 2006), *Leptospirillum* (Gihring et al., 2006; Johnson, 2012), and Cyanobacteria (Bose et al., 2020; Dutta et al., 2018; Gihring et al., 2006; Momper, Reese, et al., 2017), with the exception of *Rhodoplanes* for which this is the first report of its identification in the deep subsurface. The presence of genes encoding nitrate ammonification, denitrification, sulfur oxidation and thiosulfate reduction activities in the *Rhodoplanes* sp. T2.26MG-98 genome is sufficient to explain its development in the deep subsurface in the absence of light (Mariñán et al., 2019).

Members of the Cyanobacteria class and the *Acidithiobacillus*, *Acidovorax*, *Desulfosporosinus*, *Pseudomonas*, *Sulfobacillus* and *Tessaracoccus* genera were detected in 13 out of 19 analysed intervals, using at least three independent methodologies. As mentioned, Cyanobacteria had been previously reported in several drilling operations (Bose et al., 2020; Dutta et al., 2018; Gihring et al., 2006; Momper, Reese, et al., 2017) and in samples from borehole BH10 (Puente-Sánchez et al., 2018), indicating the existence of non-photosynthetic alternative metabolisms, such as the use of H₂, in this important group of microorganisms. Moreover, we have previously isolated and characterized an endogenous IPB subsurface nitrate-reducing bacterium from the same drilling, *Tessaracoccus lapidicaptus* (Puente-Sánchez, Sánchez-Román, et al., 2014). Members of this genus must have an important role in the subsurface of the IPB because they have been detected at different depths using diverse independent methodologies and identified in all sequenced enrichment cultures (Dataset S7).

Furthermore, *Acidovorax*, *Pseudomonas* and *Rhizobium* correspond to a core terrestrial deep subsurface bacteria of eight genera (*Acidovorax*, *Diaphorobacter*, *Deffluvimonas*, *Palnomicrobium*, *Pseudomonas*, *Rhizobium*, *Rhodoferrax* and *Thauera*) selected using the sequence diversity of eight drilling operations from different lithological and geographical

locations (Soares et al., 2019). In our case, 2 of the selected genera, *Acidovorax* and *Pseudomonas*, were detected by 3 independent methods in 13 of the 19 analyzed depth intervals, and *Rhizobium* was identified by 4 different methodologies in 10 depth intervals of the deep subsurface of the IPB. *Rhodoferrax* has been detected in BH10 borehole at only one depth, 352 mbs, by means of cloning.

Twenty-nine bacteria belonging to the Pseudomonadota (*Brevundimonas*, *Desulfovibrio*, *Lelliottia*, *Pseudomonas* [five isolates], *Rhizobium* [two isolates], *Rhodoplanes* [three isolates], *Shewanella* and *Xanthobacter*), Actinomycetota (*Aestuariimicrobium*, *Cellulomonas* [two isolates], *Microbacterium*, *Nocardoides*, *Propionisimonas* and *Tessaracoccus* [four isolates]), Bacillota (*Acetoanaerobium*, *Bacillus* and *Paenibacillus*) and Bacteroidota (*Macellibacteroides*) phyla were isolated from the most active hydrogenotrophic methanogenic and autotrophic denitrifying enrichment cultures under strict anaerobic conditions (Table S6) (Leandro, 2018; Leandro et al., 2018). Most of these bacterial genera have been identified previously in the deep subsurface (*Brevundimonas*, Onstott et al., 2009; *Bacillus*, Zhang et al., 2005; *Cellulomonas*, Fry et al., 2009; *Desulfovibrio*, Motamedi & Pedersen, 1998; *Microbacterium*, Onstott et al., 2009; *Nocardoides*, Purkamo et al., 2020; *Paenibacillus*, Purkamo et al., 2020; *Pseudomonas*, Boivin-Jahns et al., 1996; *Rhizobium*, Zhang et al., 2005; *Shewanella*, Onstott et al., 2009; and *Tessaracoccus*, Cockell et al., 2012), but for some of them (*Acetoanaerobium*, *Aestuariimicrobium*, *Lelliottia*, *Macellibacteroides* and *Xanthobacter*), this is the first time that have been identified and isolated from continental hard rock deep subsurface. Currently, they are being characterized genotypically and phenotypically to better understand their role in the continental deep subsurface microbiome.

Identifying the most representative microorganisms in the subsurface of the IPB made it possible to evaluate their correlation with the minerals identified in the ecosystem and their metallic content (Figure 4). A positive correlation was observed for members of *Arthrobacter*, *Acidovorax*, *Pseudomonas*, *Rhodoplanes*, and *Sulfobacillus* genera with Fe and pyrite, in addition, two of them, *Acidovorax* and *Pseudomonas*, can oxidize Fe²⁺ in anaerobic conditions. *Acidiphilium*, an iron reducer, and *Tessaracoccus*, an iron oxidizer, showed a correlation with Cu and clinocllore, a phyllosilicate with Fe; *Brevundimonas* with Zn and illite, another phyllosilicate with Fe; *Shewanella*, an Fe reducer, with siderite, a ferrous carbonate; and *Bacillus* with Mn. Thus, most of the identified representative microorganisms in the deep subsurface of the IPB correlate with primary and secondary Fe minerals and/or elements present in the metallic sulfides existing in the IPB, underlying the intimate relationship between the identified microbial diversity and the Fe mineralogy existing in the IPB.

The activation of Fe oxidation in anaerobic conditions after the addition of water to three dry core samples with high pyrite content could be visualized as the formation of Fe^{3+} precipitates, which strongly suggest the existence of anaerobic Fe-oxidizing activities in the subsurface of the IPB (Figure S7). A metabolic reaction of importance not only in this ecosystem but also in applied biotechnological processes such as biohydrometallurgy, in which anoxic conditions are generated in the bioleaching heaps because of the exhaustion of O_2 by the aerobic respiring microorganisms, among them the Fe oxidizers (Malki et al., 2006). Isolates from four representative genera identified in the BH10 core samples, *Acidovorax*, *Tessaracoccus*, *Pseudomonas* and *Shewanella* showed efficient oxidation of ferrous iron using nitrate as electron acceptor for anaerobic respiration (Table S9). This activity could also be visualized through fluorescence microscopy of native subsurface samples by the co-occurrence of ferric iron, the oxidation product, and the presence of nitrate-reducing microorganisms, *Acidovorax* and *Tessaracoccus*, clearly identified by CARD-FISH (Figure S8). The genomic analysis of these microorganisms showed the lack of recognizable genes associated with this metabolic activity (Carlson et al., 2013; Leandro et al., 2017; Martínez et al., 2020; Mateos et al., 2022; Puente-Sánchez, Pieper, & Arce-Rodríguez, 2016), so we have to conclude that the observed oxidation of iron, at least for the tested microorganisms, is due to the chemical oxidation of Fe promoted by the high oxidizing capacity of nitrite and nitric oxide generated by the use of nitrate as electron acceptor. These results strongly support the notion that some nitrate reducers can efficiently generate reactive nitrogen species able to oxidize iron under strict anaerobic conditions (Bryce et al., 2018; Carlson et al., 2013; Straub et al., 2004).

Remarkably, 82% of the most representative genera identified in this work have been described as putative nitrate reducers. In fact, we have identified the presence of genes coding for nitrate reduction in eight of the nine sequenced genomes isolated from the IPB subsurface. This result, together with the Fe^{2+} oxidation capacity shown by some IPB isolates, strongly suggests the importance of this metabolic activity in the IPB subsurface, the origin of the high concentration of secondary Fe minerals and the presence of soluble Fe along the column as the source of the high concentration of iron detected in the Tinto basin (Allman et al., 2021; Fernández-Remolar et al., 2018). Recently, the interaction of members of the *Acidovorax* genus with pyrite in the subsurface of the IPB and the correspondent Raman spectral change of this mineral associated with this interaction has been reported (Escudero et al., 2021). In addition, preliminary experiments performed in our laboratory showed that *Acidovorax* is able to solubilize Fe from pyrite using acetate as a source of energy and nitrate as electron acceptor

(Escudero, 2018). Further research is needed to clarify the role of nitrate reduction Fe oxidation activities (NRF_{FeOx}) in the subsurface of the IPB as well as other environments.

Given the impossibility of generating useful metagenomic information from the retrieved DNA samples, and in order to obtain data on the enzymatic activities associated with the different biogeochemical cycles operating in the deep subsurface of the IPB, we have annotated the genome sequences of nine IPB subsurface isolates (*Brevundimonas* sp. T2.26MG-97, *Desulfosporosinus meridei* DEEP, *Pseudomonas* sp. T2.31D.1, *Rhizobium* sp. T2.30D-1.1, *Rhizobium* sp. T2.26MG-112.2, *Rhodoplanes* sp. T2.26MG-98, *Shewanella* sp. T2.3D-1.1, *Tessaracoccus* sp. T2.5-30 and *Tessaracoccus lepidicaptus* IPBSL-7), and the shotgun metagenomic data for Cyanobacteria, all of them belonging to the most representative genera of this ecosystem. The complete set of genes coding for the enzymatic activities able to functionally maintain the carbon cycle (CO_2 fixation, CO_2 production through respiration and fermentation), the hydrogen cycle (H_2 production and H_2 oxidation), the nitrogen cycle (N_2 fixation, dissimilatory nitrate reduction to ammonia (DNRA), nitrate reduction, denitrification), iron reduction and the sulfur cycle (S oxidation and reduction), have been detected in eight core samples obtained at different depths (Figure 5 and Table S8). The proposed roles of the most relevant identified and isolated microbial genera, their genes, and their metabolic products in the maintenance of the basic C, H, N, S and Fe biogeochemical cycles operating in a coupled mode in the deep subsurface of the IPB is shown in Figure 6. The existence of a significant number of microorganisms identified through independent methodologies at different depths, showing genes in their sequenced genomes involved in the N cycle, underscores the likely importance of this biogeochemical cycle in the subsurface, which had been previously suggested, and is confirmed by these results (Lau et al., 2014; Nuppenen-Puputti et al., 2022; Rempfert et al., 2017).

The performance and coupling of some geomicrobiological cycles in the deep subsurface have been suggested by some authors using diffused groundwater samples (Bell et al., 2020; Momper, Jungbluth, et al., 2017; Nyyssönen et al., 2014), but this is the first time that the coupling of five complete basic biogeochemical cycles is shown operating in the presence of diverse hard rock substrates at different depths, underlying the absolute need for complementary metabolisms to maintain the deep subsurface microbiome operative.

As mentioned in the Introduction, the astrobiological interest of continental subsurface life is mainly related with the search for life in other planetary bodies. The current concept of habitability, in other words, the presence of conditions that could support life in a given

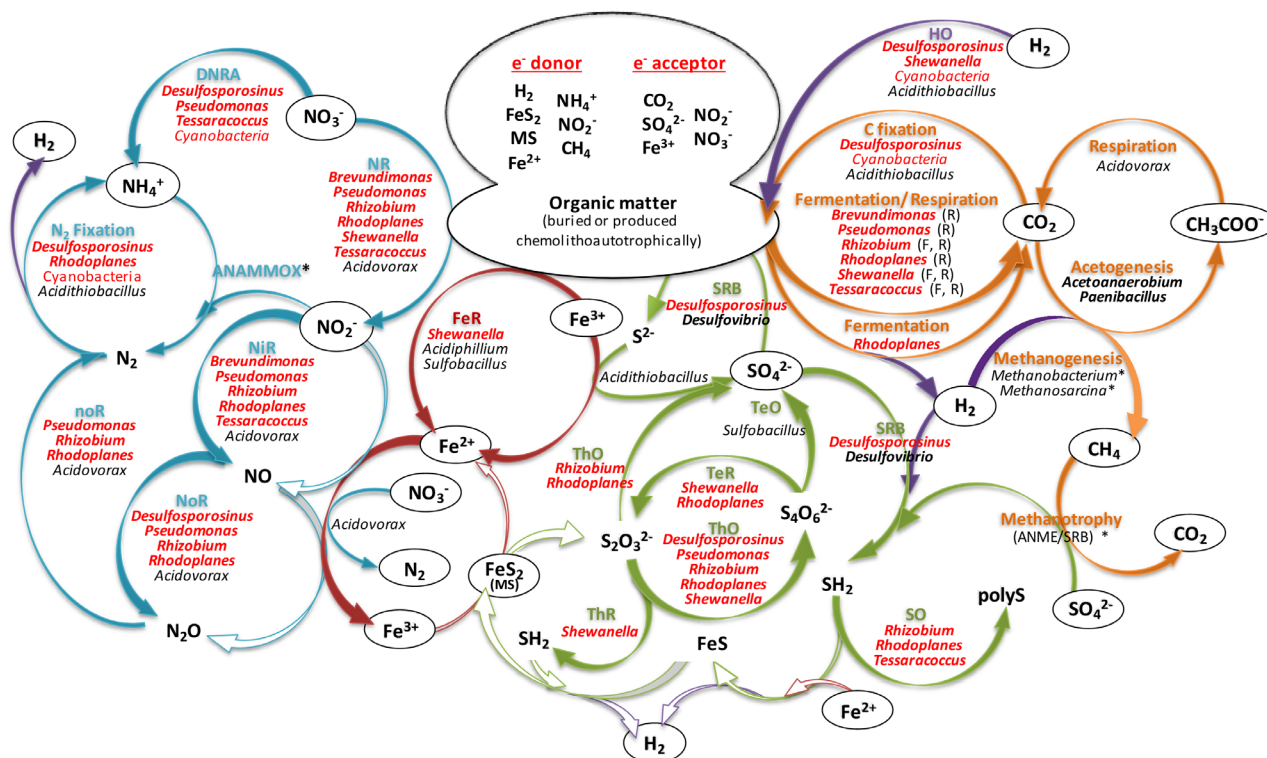


FIGURE 6 Geomicrobiological model of the C, H, N, S and Fe biogeochemical cycles operating in the deep subsurface of the IPB. Brown: C cycle; Purple: H cycle; Blue: N cycle; Green: S cycle and Red: Fe cycle. Filled arrows indicate biologically mediated reactions; hollow arrows abiotic reactions. In red: isolated genera in which the corresponding gene has been identified in their sequenced genomes; in bold-black: isolated genera without genomic information; in black: no isolated identified genera. *: genera detected by only one methodology; within black ovals: metabolites identified and quantified in this work. ANAMMOX, anaerobic ammonium oxidation; ANME, anaerobic methane oxidizing archaea; DNRA, dissimilatory nitrate reduction to ammonium; F, fermentation; FeR, iron reduction; HO, hydrogen oxidase; MS, metal sulfides; NR, nitrate reduction; NiR, nitrite reductase; NoR, nitric oxide reductase; R, respiration; SRB, sulfate reducing bacteria; SO, sulfur oxidation; TeR, tetrathionate reductase; ThO, thiosulfate oxidase, ThR, thiosulfate reductase

planet resides mainly on the detection of conditions that support the existence of liquid water on its surface (Cockell et al., 2016). Obviously, the demonstration of the existence of life in the continental deep subsurface has expanded the possible existence of life and hence the habitability of a planet by an important factor, although at this moment impossible to evaluate. A significant limitation to the estimation of the real habitability of an exoplanet is that, currently, we can only obtain information from its surface and atmosphere, and as a consequence of the distances involved, it is impossible to determine the conditions existing in their subsurface. This problem does not exist in our solar system, where exploration missions could be sent to collect sufficient information on the deep subsurface properties, or even better, to bring samples back to Earth for deeper analysis. An interesting case can be found in Mars. As the consequence of the conditions reported by diverse exploration missions, life in the surface of the planet is unlikely due to the lack of water, intense radiation, extremely oxidizing conditions and low temperature (Margulis et al., 1979; Martínez et al., 2017; Rafkin et al., 2016; Schofield et al., 1997). Definitively, the demonstration of Darwin's prediction of life in the deep

subsurface has radically changed the situation, and the next Mars missions are considering this possibility, especially after the report of liquid water in the subsurface (Orsei et al., 2018). The existence of microbial life sustaining the most important geobiological cycles in the subsurface of one mineralogical and geochemical terrestrial analogue of Mars, the IPB (Fernández-Remolar et al., 2005), allow us to conclude that the possibility of past or even extant life in the subsurface of Mars must be contemplated (Koike et al., 2020; Price et al., 2018, 2022; Purkamo et al., 2020).

CONCLUDING REMARKS

This work has identified the most represented microorganisms inhabiting the solid rock subsurface of the IPB and, together with the measured metabolic products, suggests that they carry out complete and coupled C, H, N, S and Fe biogeochemical cycles. Our results show that the IPB deep rock subsurface contains sufficient biologically accessible energy sources to support diverse microbial communities that, collectively, may amount to 4×10^{24} microbial cells, equivalent to 90 Mt

of C (Table S10). These findings favour the hypothesis of a massive underground bioreactor that contributes to the characteristic extreme conditions detected in the Río Tinto basin, thus opening a path to the identification of analogous biogeochemical cycles likely operating in other continental subsurface formations and, eventually, even in the subsurface of other planets as it is the case of Mars.

AUTHOR CONTRIBUTIONS

Ricardo Amils: Conceptualization (equal); formal analysis (equal); funding acquisition (equal); investigation (equal); project administration (equal); writing – original draft (equal). **Cristina Escudero:** Conceptualization (equal); formal analysis (equal); investigation (equal); methodology (equal); writing – review and editing (equal). **Monike Oggerin:** Formal analysis (equal); investigation (equal); methodology (equal); supervision (equal). **Fernando Puente:** Data curation (equal); formal analysis (equal); investigation (equal); visualization (equal). **Alejandro Arce-Rodríguez:** Data curation (equal); formal analysis (equal); investigation (equal); visualization (equal). **David Fernández-Remolar:** Conceptualization (equal); data curation (equal); formal analysis (equal); investigation (equal); writing – review and editing (equal). **Nuria Rodríguez:** Data curation (equal); formal analysis (equal); investigation (equal); resources (equal); visualization (equal). **Miriam García-Villadangos:** Formal analysis (equal); investigation (equal); methodology (equal). **Jose Luis Luis Sanz Martin:** Formal analysis (equal); investigation (equal); methodology (equal). **Carlos Briones:** Formal analysis (equal); investigation (equal); methodology (equal); writing – review and editing (equal). **Mónica Sánchez:** Formal analysis (equal); investigation (equal). **Felipe Gomez:** Formal analysis (equal); investigation (equal). **Tania Leandro:** Formal analysis (equal); investigation (equal); methodology (equal). **Mercedes Moreno-Paz:** Formal analysis (equal); investigation (equal). **Olga Prieto-Ballesteros:** Formal analysis (equal); investigation (equal). **Antonio Molina:** Investigation (equal). **Fernando Tornos:** Formal analysis (equal); investigation (equal). **Irene Sanchez-Andrea:** Formal analysis (equal); investigation (equal). **Kenneth Timmis:** Conceptualization (equal); formal analysis (equal); funding acquisition (equal); supervision (equal); writing – review and editing (equal). **Dietmar H. Pieper:** Formal analysis (equal); supervision (equal); writing – review and editing (equal). **Victor Parro:** Conceptualization (equal); formal analysis (equal); investigation (equal); supervision (equal); writing – review and editing (equal).

ACKNOWLEDGEMENTS

The authors thank J. P. Fernández-Rodríguez, J. A. Rodríguez-Manfredi, F. López de Saro, E. Omoregie, M. Fernández-Algar, M. Postigo, P. Cruz-Gil, Y. Blanco,

M. Fernández Sampedro, M. Martín (from the Centro de Astrobiología) and J. M. Martínez (U. Autónoma de Madrid), D. Gómez-Ortiz (U. Rey Juan Carlos), L. Loisel (Australian National U.), the Optical and Confocal Microscopy Service (CBMSO), and the Unit of Elemental Analysis (Sidi, U. Autónoma de Madrid) for their collaboration in different tasks of the project, and R. Samalot for the English correction of the manuscript. The authors thank C. Primo and A. Primo (Hotel Vázquez Díaz, Nerva, Spain), different members of the Fundación Río Tinto and the Museo Minero de Riotinto “Ernest Lluch” for their valuable collaboration in different aspects of the drilling part of the project. This work has been supported by the ERC Advance Grant #250-350 “Iberian Pyrite Belt Subsurface Life Detection” (IPBSL).

CONFLICT OF INTEREST

The authors declare that they do not have any conflict of interest.

DATA AVAILABILITY STATEMENT

All used data can be found in the manuscript or as supporting information.

ORCID

Ricardo Amils  <https://orcid.org/0000-0002-7560-1033>

REFERENCES

- Allman, C.J., Gómez-Ortiz, D., Burke, A., Amils, R., Rodríguez, N. & Fernández-Remolar, D.C. (2021) Hydrogeochemical variability of the acidic springs in the Río Tinto headwaters. *Water*, 13, 2861. Available from: <https://doi.org/10.3390/w13202861>
- Alvarez, O. & Nieto, J.M. (2015) Background conditions and mining pollution throughout history in the Río Tinto (SW Spain). *Environments*, 2, 295–316.
- Amaral-Zettler, L., Gómez, F., Zettler, E.R., Keenan, B.G., Amils, R. & Sogin, M. (2002) Eukaryotic diversity in Spain's “river of fire”. *Nature*, 417, 137.
- Amils, R. (2016) Lessons learned from thirty years of geomicrobiological studies of Río Tinto. *Research in Microbiology*, 167, 539–545.
- Amils, R., Fernández-Remolar, D., Gómez, F., González-Toril, E., Rodríguez, N., Briones, C. et al. (2008) In microbiology of extreme soils. In: Dion, P. & Nautiyal, C.S. (Eds.) *Subsurface geomicrobiology of the Iberian Pyritic Belt*. Berlin, Heidelberg: Springer, pp. 205–223.
- Barriga, F.J.A.S. (1990) Metallogenesis in the Iberian Pyrite Belt. In: Dallmeyer, R.D. & Garcia, E.M. (Eds.) *Pre-mesozoic geology of Iberia*. Berlin, Heidelberg: Springer-Verlag, pp. 369–379.
- Bastin, E.S., Greer, F.E., Merrit, C. & Moulton, G. (1926) The presence of sulfate reducing bacteria in oil field waters. *Science*, 63, 21–24.
- Bell, E., Lamminmäki, T., Alneberg, J., Andersen, A.F., Quian, C., Xiong, W. et al. (2020) Active sulfur cycling in the terrestrial deep subsurface. *The ISME Journal*, 14, 1260–1272.
- Bohorquez, L.C., Delgado-Serrano, L., López, G., Osorio-Forero, C., Klepac-Ceraj, V., Kolter, R. et al. (2012) In-depth characterization via complementing culture-independent approaches of the microbial community in an acidic hot spring of the Colombian Andes. *Microbial Ecology*, 63(1), 103–115.
- Boivin-Jahns, V., Ruimy, R., Bianchi, A., Daumas, S. & Christen, R. (1996) Bacterial diversity in a deep-subsurface clay

- environment. *Applied and Environmental Microbiology*, 62, 3405–3412.
- Bose, H., Dutta, A., Roy, A., Gupta, A., Mukhopadhyay, S., Mohapatra, B. et al. (2020) Microbial diversity of drilling fluids from 3000 mm deep Koyna pilot borehole provides insights into the deep biosphere of continental earth crust. *Scientific Drilling*, 27, 1–23. Available from: <https://doi.org/10.5194/sd-27-1-2020>
- Boston, P., Ivanov, M. & McKay, C. (1992) On the possibility of chemosynthetic ecosystems in subsurface habitats on Mars. *Icarus*, 95, 300–306.
- Breuker, A., Köweker, G., Blazejak, A. & Schippers, A. (2011) The deep biosphere in terrestrial sediments in the Chesapeake Bay area, Virginia, USA. *Frontiers in Microbiology*, 2, 156. Available from: <https://doi.org/10.3389/fmicb.2011.00156>
- Bryce, C., Blackwell, N., Schmidt, C., Otte, J., Huang, Y.M., Kleindienst, S. et al. (2018) Microbial anaerobic Fe(II) oxidation—ecology, mechanisms and environmental implications. *Environmental Microbiology*, 20, 3462–3483.
- Cabugao, K.G.M., Gushgari-Doyle, S., Chacon, S.S., Wu, X., Bhattacharyya, A., Bouskill, N. et al. (2022) Characterizing natural organic matter transformations by microbial communities in terrestrial subsurface ecosystems: a critical review of analytical techniques and challenges. *Frontiers in Microbiology*, 13, 864895.
- Camarinha-Silva, A., Jáuregui, R., Chaves-Moreno, D., Oxley, A.P.A., Schaumburg, F., Becker, K. et al. (2014) Comparing the anterior rare bacterial community of two discrete human populations using Illumina amplicon sequencing. *Environmental Microbiology*, 16(2939), 2952.
- Carlson, H.K., Clark, I.C., Blazewicz, S.J., Iavarone, A.T. & Coates, J. D. (2013) Fe(II) oxidation is an innate capability of nitrate-reducing bacteria that involves abiotic and biotic reactions. *Journal of Bacteriology*, 195, 3260–3268.
- Caspi, R., Altman, T., Billington, R., Dreher, K., Foerster, H., Fulcher, C.A. et al. (2014) The MetaCyc database of metabolic pathways and enzymes and the BioCyc collection of pathway/genome databases. *Nucleic Acids Research*, 42, 459–471.
- Chapelle, F.H., O'neil, K., Bradley, P.M., Methé, B.A., Cinfo, S.A., Knobel, L.L. et al. (2002) A hydrogen-based subsurface microbial community dominated by methanogens. *Nature*, 415, 312–315.
- Cockell, C.S., Bush, T., Bryce, C., Direito, S., Fox-Powell, M., Harrison, J.P. et al. (2016) Habitability: a revision. *Astrobiology*, 16(1), 89–117.
- Cockell, C.S., Schaefer, B., Wuchter, C., Coolen, M.J.L., Grice, K., Schnieders, L. et al. (2021) Shaping of the present-day deep biosphere at Chicxulub by the impact catastrophe that ended the Cretaceous. *Frontiers in Microbiology*, 12, 668240.
- Cockell, C.S., Voytek, M.A., Gronstal, A.L., Finster, K., Kirshtein, J.D., Howard, K. et al. (2012) Impact disruption and recovery of the deep subsurface biosphere. *Astrobiology*, 12, 231–246.
- Colman, D., Poudel, S., Stamps, B.W., Boyd, E.S. & Spear, J.R. (2017) The deep, hot biosphere: twenty-five years of retrospection. *Proceedings of the National Academy of Sciences of the United States of America*, 114, 6895–6903.
- Coyte, K.Z., Tabuteau, H., Gaffney, E.A., Foster, K.R. & Durham, W. M. (2017) Microbial competition in porous environments can select against rapid biofilm growth. *Proceedings of the National Academy of Sciences of the United States of America*, 114(2), E161–E170. Available from: <https://doi.org/10.1073/pnas.1525228113>
- Darwin, C. (1839) *Voyages of the adventure and beagle, volume III—journal and remarks, 1832–1836*. London, England: Henry Colburn.
- de Polanco, S., Martínez, J.M., Leandro, L. & Amils, R. (2020) Draft genome sequence of *Shewanella* sp. strain T2.3D-1.1 isolated from 121.8 meters deep in the subsurface of the Iberian Pyrite Belt. *Microbiology Resource Announcements*, 9, e00190–e00120.
- D'Hondt, S., Rutherford, S. & Spivack, A.J. (2002) Metabolic activity of subsurface life in deep-sea sediments. *Science*, 295, 2067–2070.
- Dubois, M., Gilles, K.A., Hamilton, J.K., Rebers, P.A. & Smith, F. (1956) Colorimetric method for determination of sugars and related substances. *Analytical Chemistry*, 28, 350–356.
- Dutta, A., Dutta Gupta, S., Gupta, A., Sarkar, J., Roy, S., Mukherjee, A. et al. (2018) Exploration of deep terrestrial subsurface microbiome in late Cretaceous Deccan traps and underlying Archean basement. *Indian Science Reports*, 8, 17459.
- Easton, A.J. (1972) The colorimetric determination of iron. In: *Analysis of silicate rocks, in methods in geochemistry and geophysics series*, Vol. 6. Amsterdam: Elsevier, pp. 95–112.
- Escudero, C. (2018) *Fluorescence microscopy for the in situ study of the Iberian Pyrite Belt subsurface geomicrobiology*. Madrid: Universidad Autónoma de Madrid.
- Escudero, C. & Amils, R. (2022) Dark biosphere: just at the very tip of the iceberg. *Environmental Microbiology*, 2022, 1–3. Available from: <https://doi.org/10.1111/1462-2920.16265>
- Escudero, C., del Campo, A., Ares, J.R., Sánchez, C., Martínez, J.M., Gómez, F. et al. (2021) Visualizing microorganisms-mineral interaction in the Iberian Pyrite Belt subsurface: the *Acidovorax* case. *Frontiers in Microbiology*, 11, 572104.
- Escudero, C., Oggerin, M. & Amils, R. (2018) The deep continental subsurface: the dark biosphere. *International Microbiology*, 21, 3–14.
- Escudero, C., Vera, M., Oggerin, M. & Amils, R. (2018) Active microbial biofilms in deep poor porous continental subsurface rocks. *Scientific Reports*, 8, 1538.
- Fernández-Remolar, D., Banerjee, N., Gómez-Ortiz, D., Izawa, M. & Amils, R. (2018) A mineralogical archive of the biogeochemical sulfur cycle preserved in the subsurface of Rio Tinto system. *American Mineralogist*, 103, 394–411.
- Fernández-Remolar, D., Morris, R.V., Gruener, J.E., Amils, R. & Knoll, A. (2005) The Rio Tinto Basin, Spain: mineralogy, sedimentary geobiology, and implications for interpretation of outcrop rocks at Meridiani planum, Mars. *Earth and Planetary Science Letters*, 240, 149–167.
- Fernández-Remolar, D., Prieto-Ballesteros, O., Rodríguez, N., Gómez, F., Amils, R., Gomez-Elvira, J. et al. (2008) Underground habitats found in the Rio Tinto Basin: a model for subsurface life habitats on Mars. *Astrobiology*, 8, 1023–1047.
- Fredrickson, J.K., Zachara, J.M., Kennedy, D.W., Dong, H., Onstott, T.C., Himman, N.W. et al. (1998) Biogenic iron mineralization accompanying the dissimilatory reduction of hydrous ferric oxide by a groundwater bacterium. *Geochimica et Cosmochimica Acta*, 62, 3229–3257.
- Fry, J.C., Horsfield, B., Skykes, R., Cragg, B.A., Heywood, C., Tae Kim, G. et al. (2009) Prokaryotic populations and activities in the interbedded coal deposit, including a previously deeply buried section (1.6–2.3 km) above ≈150 basement rock. *Geomicrobiology Journal*, 26, 163–178.
- García, R., Martínez, J.M., Leandro, L. & Amils, R. (2018) Draft genome sequence of *Rhizobium* sp. strain T2.30D-1.1 isolated from 538.5 meter deep on the Iberian Pyrite Belt subsurface. *Microbiology Resource Announcement*, 7, e01098–e01018.
- Garrido, P., González-Toril, E., Gracia-Moyano, A., Moreno-Paz, M., Amils, R., Parro, V. et al. (2008) An oligonucleotide prokaryotic acidophile microarray: its validation and its use to monitor seasonal variations in extreme acidic environments with total environmental RNA. *Environmental Microbiology*, 10, 836–850.
- Gihring, T.M., Moser, D.P., Lin, L.H., Davidson, M., Onstott, T.C., Morgan, L. et al. (2006) The distribution of microbial taxa in the subsurface water of the Kalahari Shield, South Africa. *Geomicrobiology Journal*, 23, 415–430.

- Gold, T. (1992) The deep, hot biosphere. *Proceedings of the National Academy of Sciences of the United States of America*, 89, 6045–6049.
- Gómez-Ortiz, D., Fernández-Remolar, D., Granda, A., Quesada, C., Granda, T., Prieto-Ballesteros, O. et al. (2014) Identification of the subsurface sulfide bodies responsible for acidity in Río Tinto source water, Spain. *Earth and Planetary Science Letters*, 391, 36–42.
- González-Toril, E., Llobet-Brosa, E., Casamayor, E., Amann, R. & Amils, R. (2003) Microbial ecology of an extreme acidic environment, the Río Tinto. *Applied and Environmental Microbiology*, 69, 4853–4865.
- Hugenholtz, P., Tyson, G.W. & Blackall, L.L. (2002) Design and evaluation of 16S rRNA-targeted oligonucleotide probes for fluorescence in situ hybridization. *Methods in Molecular Biology*, 179, 29–42.
- Hungate, R.E. (1969) A roll tube method for cultivation of strict anaerobes. *Journal of Microbiological Methods*, 3, 117–132.
- Itävaara, M., Nyssönen, M., Kapanen, A., Nousiainen, A., Ahonen, L. & Kukkonen, I. (2011) Characterization of bacterial diversity to a depth of 1500 m in the Outokumpu deep borehole, Fennoscandian shield. *FEMS Microbiology Ecology*, 77, 295–309.
- Johnson, D.B. (2012) Geomicrobiology of extremely acidic subsurface environments. *FEMS Microbiology Ecology*, 81, 2–12.
- Kanehisa, M. & Susumu, G. (2000) KEGG, Kyoto encyclopedia of genes and genomes. *Nucleic Acids Research*, 28(1), 27–30.
- Kappler, A., Bryce, C., Mansor, M., Lueder, U., Byrne, J.M. & Swanner, E.D. (2021) An evolving view on biogeochemical cycling of iron. *Nature Reviews. Microbiology*, 19, 360–374.
- Kappler, K., Schink, B. & Newman, D.K. (2005) Fe(III) mineral formation and cell encrustation by the nitrate-dependent Fe(II)-oxidizer strain BoFeN1. *Geobiology*, 3, 235–245.
- Knittel, K. & Boetius, A. (2009) Anaerobic oxidation of methane: progress with an unknown process. *Annual Review of Microbiology*, 63, 311–334.
- Koike, M., Nakada, R., Kajitani, I., Usui, T., Tamenori, Y., Sugahara, H. et al. (2020) In-situ preservation of nitrogen-bearing organics in Noachian Martian carbonates. *Nature Communications*, 11(1), 1988. Available from: <https://doi.org/10.1038/s41467-020-15931-4>
- Kotelnikova, S. (2002) Microbial production and oxidation of methane in deep subsurface. *Earth-Science Reviews*, 58, 367–395.
- Kozich, J.J., Westcott, S.L., Baxter, N.T., Highlander, S.K. & Schloss, P.D. (2013) Development of a dual-index sequencing strategy and curation pipeline for analyzing amplicon sequence data on the MiSeq Illumina platform. *Applied and Environmental Microbiology*, 79, 5112–5120.
- Kuenen, J.G. (2008) Anammox bacteria: from discovery to application. *Nature Reviews. Microbiology*, 6, 320–326.
- Lau, M.C.Y., Cameron, C., Magnabosco, C., Brown, T., Schilkey, F., Grim, S. et al. (2014) Phylogeny and phylogeography of functional genes shared among seven terrestrial subsurface metagenomes reveal N-cycling and microbial evolutionary relationships. *Frontiers in Microbiology*, 5, 531. Available from: <https://doi.org/10.3389/fmicb.2014.00531>
- Lau, M.C.Y., Kieft, T.L., Kuloyo, O., Linage-Alvarez, B., van Heerden, E., Lindsay, M.R. et al. (2016) An oligotrophic deep-subsurface community dependent on syntrophy is dominated by sulphur-driven autotrophic denitrifiers. *Proceedings of the National Academy of Sciences of the United States of America*, 113, E7927–E7936.
- Leandro, T. (2018) *Microbial diversity and anaerobic metabolisms in the subsurface of the Iberian Pyrite Belt*. Coimbra: Coimbra University.
- Leandro, T., da Costa, M.S., Sanz, J.L. & Amils, R. (2017) Complete genome of *Tessaracoccus* sp. strain T2.5-30 isolated from 139.5 m deep on the subsurface of the Iberian Pyrite Belt. *Gene Announcement*, 5, e00238–e00217.
- Leandro, T., Rodríguez, N., Sanz, J.L., da Costa, M.S. & Amils, R. (2018) Study of methanogenic enrichment cultures of rock cores from the deep subsurface of the Iberian Pyrite Belt. *Heliyon*, 4, e00605.
- Leblanc, M., Morales, J., Borrego, J. & Elbaz-Poulichet, F. (2000) 4500-year-old mining pollution in southwestern Spain: long-term implications for modern mining pollution. *Economic Geology*, 95, 655–662.
- Lehman, R.M., O'Connell, S.P., Banta, A., Fredrickson, J.K., Reysenbach, A.L., Kieft, T.L. et al. (2004) Microbiological comparison of core and groundwater samples collected from a fractured basalt aquifer with that of dialysis chambers incubated in situ. *Geomicrobiology Journal*, 21, 169–182.
- Lescuyer, J.L., Leistel, J.M., Marcoux, E., Milési, J.P. & Thiéblemont, D. (1998) Late Devonian-early Carboniferous peak sulphide mineralization in the Western Hercynides. *Mineralium Deposita*, 33, 208–220.
- Liu, Q., Adler, K., Lipus, D., Kämpf, H., Bussert, R., Plessen, B. et al. (2020) Microbial signatures in deep CO₂-saturated Miocene sediments of the Active Hartousov Moffett System (NW Czech Republic). *Frontiers in Microbiology*, 11, 543260. Available from: <https://doi.org/10.3389/fmicb.2020.543260>
- Lovley, D.R. & Chapelle, F.H. (1995) Deep subsurface microbial processes. *Reviews of Geophysics*, 33, 365–381.
- Ludwig, W., Strunk, O., Westram, R., Richter, L., Meier, H., Yadhukumar et al. (2004) ARB: a software environment for sequence data. *Nucleic Acids Research*, 32, 1363–1371. Available from: <https://doi.org/10.1093/nar/gkh293>
- Magnabosco, C., Lin, L.H., Dong, H., Bomberg, M., Ghiorse, W., Stan-Lotter, H. et al. (2018) The biomass and biodiversity of the continental subsurface. *Nature Geoscience*, 11, 707–717.
- Magnabosco, C., Ryan, K., Lau, M.C.Y., Kuloyo, O., Sherwood Lollar, B. & Kieft, T.L. (2016) A metagenomic window into carbon metabolism at 3 km depth in Precambrian continental crust. *The ISME Journal*, 10, 730–741.
- Malki, M., González-Toril, E., Sanz, J.L., Gómez, F., Rodríguez, N. & Amils, R. (2006) Importance of the iron cycle in biohydrometallurgy. *Hidrometallurgy*, 83, 223–228.
- Margulis, L., Mazur, P., Barghoorn, E.S., Halvorson, H.O., Jukes, T. H.J. & Kaplan, I.R. (1979) The Viking Mission: implications for life in the Vallis Marineris area. *Science*, 305, 78–81.
- Mariñán, N., Martínez, J.M., Leandro, T. & Amils, R. (2019) Draft genome sequence of *Rhodoplanes* sp. strain T2.26MG-98 isolated from 492.6 meter deep on the subsurface of the Iberian Pyrite Belt. *Microbiology Resource Announcements*, 8, e00070.
- Martínez, G.M., Newman, C.N., de Vicente-Retortillo, A., Fischer, E., Rennó, N.O., Richardson, M.I. et al. (2017) The modern near-surface martian climate: a review on insitu meteorological data from Viking to Curiosity. *Space Science Reviews*, 212, 295–338.
- Martínez, J.M., Escudero, C., Leandro, T., Mateos, G. & Amils, R. (2020) Draft genome sequence of *Pseudomonas* sp. strain T2.31D-1 isolated from 414 meters deep in the subsurface of the Iberian Pyrite Belt. *Microbiology Resource Announcements*, 11, e572104.
- Mateos, G., Martínez Bonilla, A., de Polanco, S., Martínez, J.M., Escudero, C., Rodríguez, N. et al. (2022) *Shewanella* sp. T2.3D-1.1 a novel microorganism sustaining the iron cycle in the deep subsurface of the Iberian Pyrite Belt. *Microorganisms*, 10, 1585. Available from: <https://doi.org/10.3390/microorganisms10081585>
- Miyoshi, T., Iwatsuki, T. & Naganuma, T. (2005) Phylogenetic characterization of 16 S rRNA gene clones from deep-groundwater microorganisms that pass through 0.2-micrometer-pore-size filters. *Applied and Environmental Microbiology*, 71, 1084–1088.

- Momper, L., Jungbluth, S.P., Lee, M.D. & Amend, J.P. (2017) Energy and carbon metabolisms in a deep terrestrial subsurface fluid microbial community. *The ISME Journal*, 11, 2319–2333.
- Momper, L., Reese, B.K., Zinke, L., Wanger, G., Osburn, M.R., Moser, D. et al. (2017) Major phylum-level differences between porefluid and host rock bacterial communities in the terrestrial deep subsurface. *Environmental Microbiology Reports*, 9, 501–511.
- Morita, R.Y. (1999) Is H₂ the universal energy source for long-term survival? *Microbial Ecology*, 38, 307–320.
- Motamedi, M. & Pedersen, K. (1998) *Desulfovibrio aespoensis* sp. nov., a mesophilic sulfate-reducing bacterium from deep groundwater at Äspö hard rock laboratory, Sweden. *International Journal of Systematic and Evolutionary Microbiology*, 48, 311–315.
- Nuppen-Puputti, M., Kietäväinen, R., Raulio, M., Soro, A., Purkamo, L., Kukkonen, I. et al. (2022) Eplithic microbial community functionality in deep oligotrophic continental bedrock. *Frontiers in Microbiology*, 13, 826048.
- Nyyssönen, M., Hultman, J., Ahonen, L., Kukkonen, I., Paulin, L., Laine, P. et al. (2014) Taxonomically and functionally diverse microbial communities in deep crystalline rocks of the Fennoscandian shield. *The ISME Journal*, 8, 126–138.
- Onstott, T., McGown, D.J., Bakermans, C., Ruskeeniemi, T., Ahonen, L., Telling, J. et al. (2009) Microbial communities in subpermafrost saline fracture water at the Lupin Au Mine, Nunavut, Canada. *Microbial Ecology*, 58, 786–807.
- Onstott, T., Moser, D.P., Offner, S.M., Fredrickson, J.K., Brockman, F.J., Phelps, T. et al. (2003) Indigenous and contaminant microbes in ultradeep mines. *Environmental Microbiology*, 5, 1168–1191.
- Orsei, R., Lauro, S.E., Pettinelli, E., Cicchetti, A., Coradini, M., Di Paolo, F. et al. (2018) Radar evidence of subglacial liquid water on Mars. *Science*, 361, 490–493.
- Pantke, C., Obst, M., Benzerara, K., Morin, G., Ona-Nguema, G., Dippon, U. et al. (2012) Green rust formation during Fe(II) oxidation by the nitrate-reducing *Acidovorax* sp. strain BoFeN1. *Environmental Science & Technology*, 46, 1439–1446.
- Parro, V.d., Diego-Castilla, G., Moreno-Paz, M., Blanco, Y., Cruz-Gil, P., Rodríguez-Manfredi, J.A. et al. (2011) A microbial oasis in the hypersaline Atacama subsurface discovered by a life detector chip: implications for the search of life on Mars. *Astrobiology*, 11, 969–996.
- Pedersen, K. (1993) The deep subterranean biosphere. *Earth-Science Reviews*, 34, 243–260.
- Pedersen, K. (1997) Microbial life in deep granitic rock. *FEMS Microbiology Reviews*, 20, 399–414.
- Pedersen, K. (2000) Exploration of deep intraterrestrial microbial life: current perspectives. *FEMS Microbiology Letters*, 185, 9–16.
- Pedersen, K. & Albinsson, Y. (1992) Possible effects of bacteria on trace element migration in crystalline bed-rock. *Radiochimica Acta*, 58(59), 365–369.
- Phelps, T., Murphy, E., Pfiffner, S. & White, D. (1994) Comparison between geochemical and biological estimates of subsurface microbial activities. *Microbial Ecology*, 28, 335–349.
- Poulsen, L.K., Ballard, G. & Stahl, D.A. (1993) Use of rRNA fluorescence in situ hybridization for measuring the activity of single cells in young and established biofilms. *Applied and Environmental Microbiology*, 59, 1354–1360.
- Price, A., Macey, M.C., Pearson, V.K., Schwenzer, S.P., Ramkissoon, N.K. & Olsson-Francis, S.P. (2022) Oligotrophic growth of nitrate-dependent Fe²⁺-oxidizing microorganisms under simulated early martian conditions. *Frontiers in Microbiology*, 13, 800219.
- Price, A., Pearson, V.K., Schwenzer, S.P., Miot, J. & Olsson-Francis, K. (2018) Nitrate-dependent iron oxidation: a potential Mars metabolism. *Frontiers in Microbiology*, 9, 513.
- Pruesse, E., Peplies, J. & Glöckner, F.O. (2012) SINA: accurate high-throughput multiple sequence alignment of ribosomal RNA genes. *Bioinformatics*, 28, 1823–1829.
- Pruesse, E., Quast, C., Knittel, K., Fuchs, B.M., Ludwig, W., Peplies, J. et al. (2007) SILVA: a comprehensive online resource for quality checked and aligned ribosomal RNA sequence data compatible with ARB. *Nucleic Acids Research*, 35, 7188–7196.
- Puente-Sánchez, F., Aguirre, J. & Parro, V. (2016) A novel conceptual approach to read-filtering in high-throughput amplicon sequencing studies. *Nucleic Acids Research*, 44(4), e40. Available from: <https://doi.org/10.1093/nar/gkv1113>
- Puente-Sánchez, F., Arce-Rodríguez, A., Oggerin, M., García-Villadangos, M., Moreno-Paz, M., Blanco, Y. et al. (2018) Viable cyanobacteria in the deep continental subsurface. *Proceedings of the National Academy of Sciences of the United States of America*, 115, 10702–10707.
- Puente-Sánchez, F., Moreno-Paz, M., Rivas, L., Cruz-Gil, P., García-Villadangos, M., Gómez, M.J. et al. (2014) Deep subsurface sulfate reducing and methanogenesis in the Iberian Pyrite Belt revealed through geochemistry and molecular biomarkers. *Geobiology*, 12, 34–37.
- Puente-Sánchez, F., Pieper, D.H. & Arce-Rodríguez, A. (2016) Draft genome sequence of the deep-subsurface Actinobacterium *Tessaracoccus lapidicaptus* IPBSL-7^T. *Gene Announcement*, 4(5), e01078–e01016.
- Puente-Sánchez, F., Sánchez-Román, M., Amils, R. & Parro, V. (2014) *Tessaracoccus lapidicaptus* sp. nov., an actinobacterium isolated from the deep subsurface of the Iberian Pyrite Belt. *International Journal of Systematic and Evolutionary Microbiology*, 64, 3546–3552.
- Purkamo, L., Bomberg, M., Nyyssönen, M., Ahonen, L., Kukkonen, I. & Itävaara, M. (2017) Response of deep subsurface microbial community to different carbon sources and electron acceptors during 2 months incubation in microcosms. *Frontiers in Microbiology*, 8, 232. Available from: <https://doi.org/10.3389/fmicb.2017.00232>
- Purkamo, L., Kietäväinen, R., Miettinen, H., Sohlberg, E., Kukkonen, I., Itävaara, M. et al. (2018) Diversity and functionality of archaeal, bacterial and fungal communities in deep Archean bedrock groundwater. *FEMS Microbiology Ecology*, 94, 8. Available from: <https://doi.org/10.1093/femsec/fiy116>
- Purkamo, L., Kietäväinen, R., Nuppen-Puputti, M., Bomberg, M. & Cousins, C. (2020) Ultradeep microbial communities at 4.4 km within crystalline bedrock: implications for habitability in planetary context. *Life*, 10, 2. Available from: <https://doi.org/10.3390/life10010002>
- Quast, C., Pruesse, E., Yilmaz, P., Gerken, J., Schweer, T., Yarza, P. et al. (2013) The SILVA ribosomal RNA gene database project: improved data processing and web-based tools. *Nucleic Acids Research*, 41, D590–D596.
- Rafkin, S.C.R., Pla-García, J., Kahre, M.A., Gómez-Elvira, J., Hamilton, V.E., Marín, M. et al. (2016) The meteorology of gale crater as determined from rover environmental monitoring station observations and numerical modeling. Part II. *Icarus*, 280, 114–138.
- Rempfert, K.R., Miller, H.M., Bompard, N., Nothaf, D., Matter, J.M., Kelemen, P. et al. (2017) Geological and geochemical controls on subsurface microbial life in the Samail Ophiolite, Oman. *Frontiers in Microbiology*, 8, 56.
- Rodríguez-Robles, E., Martínez, J.M., Leandro, T. & Amils, R. (2019) Draft genome of *Brevundimonas* sp. strain T2.26MG-97, isolated from a rock core sample from 492.6 m deep on the subsurface of the Iberian Pyrite Belt. *Microbiology Resource Announcements*, 8, e00375–e00319.
- Rognes, T., Flouri, T., Nichols, B., Quince, C. & Mahé, F. (2016) VSEARCH: a versatile open source tool for metagenomics. *PeerJ*, 4, e2584.

- Sanz, J.L., Rodríguez, N. & Amils, R. (1997) Effect of chlorinated aliphatic hydrocarbons on the acetoclastic methanogenic activity of granular sludge. *Applied Microbiology and Biotechnology*, 47, 324–328.
- Sanz, J.L., Rodríguez, N., Escudero, C., Carrizo, D. & Amils, R. (2021) Biological production of H₂, CH₄ and CO₂ in the deep subsurface of the Iberian Pyrite Belt. *Environmental Microbiology*, 23(7), 3913–3922.
- Sauer, K. (2003) The genomics and proteomics of biofilm formation. *Genome Biology*, 4, 219. Available from: <https://doi.org/10.1186/gb-2003-4-6-219>
- Saville, R.M., Rakshe, S., Haagensen, J.A., Shukla, S. & Spormann, A.M. (2011) Energy-dependent stability of *Shewanella oneidensis* MR-1 biofilms. *Journal of Bacteriology*, 193, 3257–3264.
- Schindelin, J., Arganda-Carreras, I., Frise, E., Kaynig, V., Longair, M., Pietzsch, T. et al. (2019) Fiji: an open-source platform for biological-image analysis. *Nature Methods*, 9, 676–682.
- Schloss, P.D., Gevers, D. & Westcott, S.L. (2011) Reducing the effects of PCR amplification and sequencing artifacts on 16 S rRNA-based studies. *PLoS One*, 6(12), e27310.
- Schnakenberg, A., Aromokoeye, D.A., Kulkarni, A., Maier, L., Wunder, L.C., Richter-Heitmann, T. et al. (2021) Electron acceptor availability shapes anaerobically methane oxidizing archaea (ANME) communities in South Georgia sediments. *Frontiers in Microbiology*, 12, 617280. Available from: <https://doi.org/10.3389/fmicb.2021.617280>
- Schofield, J.T., Barnes, J.R., Crisp, D., Haberle, R.M., Larsen, S., Magalhães, J.A. et al. (1997) The Mars pathfinder atmospheric structure investigation/meteorology (ASI/MET). *Science*, 278, 1752–1758.
- Seemann, T. (2014) Prokka: rapid prokaryotic genome annotation. *Bioinformatics*, 30, 2068–2069.
- Sheik, C.S., Reese, B.K., Twing, K.I., Sylvan, J.B., Grim, S.L., Schrenk, M.O. et al. (2018) Identification and removal of contaminant sequences from Ribosomal Gene Databases: lessons from the census of deep life. *Frontiers in Microbiology*, 9, 840.
- Sherwood Lollar, G.S., Warr, O., Telling, J., Osburn, M.R. & Sherwood Lollar, B. (2019) “Follow the water”: hydrogeochemical constraints on microbial investigations 2.4 km below surface at the Kidd Creek Deep Fluid and Deep Life Observatory. *Geomicrobiology Journal*, 36, 859–872.
- Shimizu, S., Akiyama, M., Ishijima, Y., Hama, K., Kunimaru, T. & Naganuma, T. (2006) Molecular characterization of microbial communities in fault-bordered aquifers in the miocene formation of northernmost Japan. *Geobiology*, 4, 203–213.
- Shuster, J., Southam, G. & Reith, F. (2019) Applications of scanning electron microscopy in geomicrobiology. In: Kenney, J., Veeramani, H. & Alessi, D. (Eds.) *Analytical geomicrobiology: a handbook of instrumental techniques*. Cambridge: Cambridge University Press, pp. 148–165.
- Sim, K., Cox, M.J., Wopereis, H., Martin, R., Knol, J., Li, M. et al. (2012) Improved detection of Bifidobacteria with optimised 16 S rRNA-gene based pyrosequencing. *PLoS One*, 7(3), e32543.
- Smith, P.K., Krohn, R.I., Hermanson, G.T., Mallia, A.K., Gartner, F.H., Provenzano, M.D. et al. (1985) Measurement of proteins using bicinchoninic acid. *Analytical Biochemistry*, 150, 76–85.
- Soares, A., Edwards, A., An, D., Bagnoud, A., Bomberg, M., Budwill, S.M. et al. (2019) A global perspective on microbial diversity in the terrestrial deep subsurface. *bioRxiv*. Available from: <https://doi.org/10.1101/602672>
- Stevens, T. & McKinley, J. (1995) Lithoautotrophic microbial ecosystems in deep basalt aquifers. *Science*, 270, 450–455.
- Straub, K.L., Schönhuber, W.A., Buchholz-Cleven, B.E. & Schink, B. (2004) Diversity of ferrous-iron oxidizing, nitrate-reducing bacteria and their involvement in oxygen-independent iron cycling. *Geomicrobiology Journal*, 21, 371–378.
- Strous, M., Pelletier, E., Mangenot, S., Rattei, T., Lehner, A., Taylor, M.W. et al. (2006) Deciphering the evolution and metabolism of an anammox bacterium from a community genome. *Nature*, 440, 790–794.
- Suzuki, S., Ishii, S., Wu, A., Cheung, A., Tenney, A., Wanger, G. et al. (2013) Microbial diversity in The Cedars, an ultrabasic, ultrareducing and low salinity serpentinizing ecosystem. *Proceedings of the National Academy of Sciences of the United States of America*, 110, 15336–15341.
- Takai, K., Moser, D.P., DeFlaun, M., Onstott, T.C. & Fredrickson, J.K. (2001) Archaeal diversity in waters from deep South African gold mines. *Applied and Environmental Microbiology*, 67, 5750–5760.
- Tikhonov, M., Leach, R.W. & Wingreen, N.S. (2015) Interpreting 16 S metagenomic data without clustering to achieve sub-OUT resolution. *The ISME Journal*, 9, 68–80.
- Tornos, F. (2006) Environment of formation and styles of volcanogenic massive sulfides: the Iberian Pyrite Belt. *Ore Geology Reviews*, 28, 259–307.
- van Geen, A., Adkins, J.F., Boyle, E.A., Nelson, C.H. & Palenques, A. (1997) Contamination from mining of the Iberian pyrite belt. *Geology*, 25, 291–294.
- Vera, M., Schippers, A. & Sand, W. (2013) Progress in bioleaching: fundamentals and mechanisms of bacterial metal sulfide oxidation-part A. *Applied Microbiology and Biotechnology*, 97, 7529–7541.
- Woyke, T., Sczyrba, A., Lee, J., Rinke, C., Tighe, D., Clingenpeel, S. et al. (2011) Decontamination of MDA reagents for single cell whole genome amplification. *PLoS One*, 6, e26161.
- Wu, X., Holfeldt, K., Hubalek, V., Lundin, D., Aström, M., Bertilsson, S. et al. (2016) Microbial metagenomes from three aquifers in the Fennoscandian shield terrestrial deep biosphere reveal metabolic partitioning among populations. *The ISME Journal*, 10, 1192–1203.
- Zhang, G., Dong, H., Xu, Z., Zhao, D. & Zhang, C. (2005) Microbial diversity in ultra-high-pressure rocks and fluids from the Chinese Continental Drilling Project in China. *Applied and Environmental Microbiology*, 71, 3213–3227.
- Zobell, C.E. (1938) Studies on the bacterial flora of marine bottom sediments. *Journal of Sedimentary Research*, 8, 10–18.

SUPPORTING INFORMATION

Additional supporting information can be found online in the Supporting Information section at the end of this article.

How to cite this article: Amils, R., Escudero, C., Oggerin, M., Puente Sánchez, F., Arce Rodríguez, A., Fernández Remolar, D. et al. (2022) Coupled C, H, N, S and Fe biogeochemical cycles operating in the continental deep subsurface of the Iberian Pyrite Belt. *Environmental Microbiology*, 1–26. Available from: <https://doi.org/10.1111/1462-2920.16291>